

Title	MEASUREMENT OF ULTRASOUND VELOCITY IN GASES UNDER HIGH PRESSURES
Author(s)	Kimura, Masaki
Citation	大阪大学, 1987, 博士論文
Version Type	VoR
URL	<a href="https://hdl.handle.net/11094/934">https://hdl.handle.net/11094/934</a>
rights	
Note	

*Osaka University Knowledge Archive : OUKA*

<https://ir.library.osaka-u.ac.jp/>

Osaka University

MEASUREMENT OF ULTRASOUND  
VELOCITY IN GASES  
UNDER HIGH PRESSURES

MASAKI KIMURA

## Abstract

In this thesis, a piston-cylinder apparatus using gases, which can produce hydrostatic pressures up to 4 GPa and temperatures up to 800 °C is first described. The high-pressure tapered cylinder made of 350 maraging steel is 262 mm long and has a 19 mm inside diameter and a working space of 100 mm in length at 4 GPa. The support ring is made of 300 maraging steel and approximately 180 mm in thickness and 420 mm in outside diameter. For the measurements of the pressures and temperatures, a manganin gauge and a thermocouple are respectively placed inside of the tapered cylinder. No difficulty is encountered with any of these components at pressures up to 3.5 GPa, which is the world record of the gas high pressure until today. This apparatus could be used almost indefinitely, since neither a considerable change of the bore nor surface cracks in the tapered cylinder had been found thus far.

In the second part of this paper are described some experiments using the high pressure apparatus. The freezing points of nitrogen and krypton at room temperature are determined from the volume and ultrasound velocity changes. The ultrasound velocity of neon is also measured up to 3.5 GPa. Taking account of the results of the ultrasound velocity and the volume measurements, new empirical formulae for the pressure dependence of ultrasound velocities of helium, neon, argon, krypton and xenon are proposed. In addition, the phase diagram of krypton and helium gas mixture under high pressures up to 1.6 GPa at room temperature is newly obtained from the sound velocity measurement. The results of the present experiment require some corrections for the results obtained by former investigators.

## Contents

§1	Introduction	
1.1	High pressure industrial application -----	1
1.2	Solid apparatus -----	2
1.3	High-pressure gas apparatus -----	4
1.4	Measurement of ultrasound wave in gases -----	6
§2	Apparatus	
2.1	Technique and main apparatus -----	12
2.2	High-pressure tapered cylinder -----	12
2.3	Support ring -----	13
2.4	Piston and piston packings -----	14
2.5	Bottom closure and bottom packings -----	15
2.6	Preliminary gas system -----	16
§3	Experimental Procedure	
3.1	Assembly of the pressure apparatus -----	27
3.2	Measurement of pressure -----	28
3.3	Measurement of temperature -----	29
3.4	Measurement of ultrasound wave velocity -----	30
3.5	Measurement of volume -----	32
§4	Measurement of Freezing Point and Phase-Separation	
4.1	Detection of freezing point -----	42
4.2	Detection of phase separation -----	43
4.3	Phase diagram -----	47
§5	Results	
5.1	Experimental results of gas apparatus -----	53
5.2	Discussion on strength of the cylinder -----	53
5.3	Freezing point of nitrogen and krypton gas at room temperature -----	55

5.4	Velocity of ultrasound wave in pure neon gas up to 3.5 GPa -----	58
5.5	Velocity of ultrasound wave in mixture of krypton-helium gas -----	60
5.6	Phase separation and phase diagram of mixture of krypton-helium gas -----	61
ξ6	Conclusion -----	87
	Acknowledgements -----	89
	References -----	90

## §1 Introduction

Early in this century, P. W. Bridgman started his monumental contribution to high pressure research, which dominated the literature in the period up to his death in 1961. Bridgman discussed the historical development of high pressure physics and chemistry in his general review article and text book,<sup>1)</sup> which will be frequently referred to in the following chapters.

### 1.1 High pressure industrial application

The first commercial use of high pressure was in the chemical industry and particularly in the synthesis of ammonia. Le Chatelier in 1901 was the first to get hydrogen and nitrogen to combine at pressure in contact with catalyst. In the later investigations, equilibrium of 3:1 hydrogen/nitrogen mixture were studied, which showed the potential advantage of raising pressure for the synthesis. The first synthetic ammonia plant was set up in 1913, and the present annual world capacity for synthesis of ammonia is still increasing remarkably.

Perhaps the most important high pressure chemical process is the production of polyethylene. The discovery of polyethylene was described by Manning.<sup>2)</sup> After improvement of the equipment, the production of polyethylene increased enormously, and today the products are used for various purposes in the forms of film and sheet, paper coating, injection moulding, pipes and wire and cable insulation.

High pressure metal working processes were extensively studied. The use of high pressure for extrusion and drawing of

tubes, plates and rods was first proposed in 1893. Many valuable and useful reviews have been published.<sup>3,4)</sup> Isostatic compaction and hot isostatic compaction using helium and argon gas and some liquids were found to be useful and applied extensively to the process of sintering.

Pulsed and continuous high velocity water jets produced by a high pressure drop across a nozzle were used for jet cutting, disintegration of brittle materials and jet cleaning.

Experience with high pressure apparatus designs<sup>5)</sup> has shown clearly that geometry and stress distribution are fully as important as the nominal strength of the materials used. In thick-walled cylinders, application of pressure to the inside wall produces greater hoop tension stress at the inner wall. The maximum confining strength of a thick-walled cylinder may be attained by prestressing the wall material under compression. Historically this was first done on guns by wrapping them with high-strength piano wire under tension. A second way was to make the pre-stressed cylindrical wall of two or more concentric layers. A third method was 'autofrettage'. A fourth example of proper distribution of hoop stress with radius was an ingenious one by Bridgman<sup>6)</sup>, as shown by a broken circle in Fig. 1.

Boyd and Engrand<sup>7,8)</sup> designed a multiple-wall, piston-cylinder apparatus for geophysical research. Similar designs have been used by a number of researchers.<sup>9-11)</sup>

## 1.2 Solid apparatus

If the idea of a cylindrical part of a pressure vessel is

abandoned entirely, the pressure vessel walls must be the faces of an array of truncated conical or pyramidal pistons.

The simplest possible device of this kind was developed and used by Bridgman.<sup>12)</sup> The pressurized region was bounded by the flat faces of opposed, truncated pistons and by a thin, deformable gasket which was pinched between the rims of the piston faces. Apparatus of this kind worked easily up to 10 GPa, and with some difficulties up to about 20 GPa, depending upon the values of force/area ratio.

A further increase of pressure can be achieved by applying supporting stresses to the anvil franks. This type was developed by Balchan and Drickamer.<sup>13)</sup> Higher pressures were obtained by Bundy<sup>14,15)</sup> in this apparatus by fabricating the anvils with tips of sintered diamond.

The form of the Bridgman anvil which has revolutionised ultra-high pressure experimentation is the diamond-window cell, in which two single crystals of diamond (of about 1/5 - 1/2 carat) form miniature, opposed anvil. The design was developed independently at the University of Chicago<sup>16,17)</sup> and the National Bureau of Standards.<sup>18,19)</sup> A diamond flat-face anvil arrangement<sup>20)</sup> was shown in Fig. 2. Pressures over 170 GPa could be achieved with this apparatus.<sup>21)</sup>

Advantage of both piston-cylinder and anvil devices can be incorporated into single design, such as Hall's 'belt apparatus'.<sup>22)</sup> The obvious advantage of this design over Bridgman anvil is the much larger volume which can be compressed.

Another approach to compression of relatively large volumes is through the use of multiple anvils in a symmetric arrangement.



Hall<sup>23)</sup> developed the tetrahedral press in 1958, and design for cubic presses appeared soon after.<sup>24,25)</sup> A modification of the original Hall tetrahedral apparatus, was made at the U. S. National Bureau of Standards.<sup>26)</sup> This arrangement devised only one hydraulic ram, or press, which pushed downward on the top piston of the array.

Van Platen<sup>27)</sup> and Kawai<sup>28-30)</sup> built multi-anvil presses (split-sphere apparatus). Especially, the latter devised various split types of anvils and successfully brought them into practical uses. Multiple-anvil sliding systems (MASS) have been developed in both France<sup>31,32)</sup> and Japan.<sup>33-35)</sup>

In order to achieve the higher pressures and/or larger volumes, these solid apparatus of many types were remarkably developed, but gas apparatus was scarcely developed from Bridgman's piston-cylinder one.

### 1.3 High-pressure gas apparatus

The high-pressure gas apparatus is a very important tool for studying reactions; gas-gas, gas-liquid, and gas-solid. It also provides data on molecular forces from the equations of states in the condensed gas systems. Using the gas apparatus, one can investigate not only the properties of gases, but also of most kinds of more condensed materials such as liquids and solids. With inert gases as the pressure medium it is possible to obtain data at high temperatures without any reaction products from the samples. Another advantage of the gas apparatus is that a pure hydrostatic pressure can be applied to solid materials which otherwise cannot release the shear stress components. It is

suitable for chemical synthesis, other chemical reactions of materials in any form and also for measurements of both the electrical and thermal properties of materials, since the insulation of the materials from the surroundings is much easier than in the apparatuses of other types.

As for a piston-cylinder gas apparatus, Bridgman<sup>6)</sup> described a system for producing fluid-pressure up to 3 GPa in a space approximately 1/2 inch in diameter and 6 inches in length ; since then, Birch and Robertson<sup>36)</sup> developed this design and extended the cylinder bore to 3/4 inches. Hughes and Nishitake<sup>37)</sup> developed a similar gas apparatus with the same cylinder bore, and Nishitake and Hanayama<sup>38)</sup> improved this system and measured ultrasound velocity of helium, argon and nitrogen. Newhall<sup>39)</sup> reported another improved apparatus, which is now commercially available. Liebenberg, Mills and Bronson<sup>40)</sup> described a cylinder apparatus with a tungsten carbide and steel multiple-wall. In almost all the cases mentioned above, the maximum pressures obtained were less than 2.5 GPa, owing to the difficulty in finding proper materials for high-pressure vessels.

Recent progress in material science makes it possible to fabricate the vessels tolerable for pressures above 3 GPa. Lavergne and Whalley<sup>41)</sup> described steel vessels up to 5 GPa, using naphtha as the transmitting medium of pressure.

In 1978 when this project began ultrasound wave velocities had been measured only up to pressures of 2 GPa. In the spring of 1978, Professor T. Nishitake decided to build a 4 GPa apparatus in order to study the gas-gas equilibrium at higher pressures. This program was aimed at precision measurement of both pressure

and temperature of gases including mixed gases up to static pressure approaching 4 GPa at around 1000 °C. This gas apparatus is shown in Photo.1. The cylinders could be used indefinitely without changing the dimensions of seal ring. In principle, this apparatus is similar to that of Bridgman, but the value of the wall ratio, that is the ratio of outer and inner diameter, is 6. This value is much larger than 3 to 4 employed by Bridgman and many other investigators and found to be quite effective to prevent enlargement of the bore when subjected to high pressure.<sup>42)</sup>

#### 1.4 Measurement of ultrasound wave in gases

Measurements of the velocity of ultrasound waves in gases is very useful for studying their physical properties under high pressure. It directly indicates not only the adiabatic compressibility but also the phenomena of phase-changes in gases. For example, it is easy to determine the condensation and the freezing points of gases from the changes in the ultrasound velocity.

High-pressure measurements of condensed gases are invaluable in developing and testing intermolecular potentials. Recent interests in the pressure-volume-temperature properties of the gas and solid have centered around the transition from a molecular solid to a metallic solid, which occurs at sufficiently high pressures as, for example, in the interior of the planet Jupiter. There is additional interest in the ignition of hydrogen isotope pellets driven by laser pulses. In understanding the creation of a plasma from a cold target pellet, pressure-volume-

temperature data on molecular gases up to high pressures and temperatures are needed.

Mills, Liebenberg and Bronson published a series of interesting papers on the high-pressure measurements of gases, including the melting phenomena. A piston-cylinder apparatus and a study of the melting point and the ultrasound velocity of argon up to 1.3 GPa was reported.<sup>40)</sup> The melting phenomena of nitrogen<sup>43,44)</sup> was observed up to 2.2 GPa. Ultrasound velocities of hydrogen<sup>45,46)</sup>, deuterium<sup>46-48)</sup> and helium<sup>49)</sup> were measured up to 2 GPa. The melting point of ammonia<sup>50,51)</sup> was measured up to 1.4 GPa.

The phase separation effect was predicted by Van der Waals, in 1894 from the fold theory,<sup>52)</sup> and discussed in detail by Kamerlingh Onnes and Keesom in 1907.<sup>53)</sup> From the study of the free-energy surface of mixture, they suggested that, under certain conditions, a phase separation could occur at temperatures well above the critical temperatures of both components, and proposed the expression, gas-gas equilibrium. The existence of this effect was verified in 1940 for the system  $\text{NH}_3\text{-N}_2$  by Krichevskii<sup>54)</sup>. Krichevskii and later Tsiklis have found other interesting examples of this phenomenon. Reviews of experimental results were published.<sup>55,56)</sup>

Since the first success by Arons and Diepen<sup>57)</sup> in the gas-gas separation in helium-xenon mixture under high pressure, many papers have been published.<sup>58-60)</sup> Schneider<sup>58)</sup> reviewed high pressure thermodynamics of fluid mixtures. Streett<sup>59)</sup> and Tsiklis<sup>60)</sup> published reviews of equilibria in fluid mixtures. But, there scarcely exist the data available at high pressures

above 1 GPa.

From the measurement of ultrasound wave, it is possible to detect the phase-separation of a mixture of gases under high pressure. If we use two sound chambers to measure the velocity in the upper and lower part of a high-pressure cylinder, the discordance of the velocities between them show the phase-separation because of the condensation taking place in the lower part.

This paper describes the construction and the test of the gas-apparatus, using mainly neon or helium as the transmitting medium up to 3.5 GPa. The freezing points of nitrogen and krypton at room temperature were determined from the volume and ultrasound velocity changes. The experimental procedures and data of the volume and the ultrasound velocity at room temperature on nitrogen up to 2.6 GPa, neon up to 3.5 GPa, krypton up to 850 MPa, are mentioned and discussed in detail, respectively. This sort of measurement at gas pressure of 3.5 GPa is a maximum pressure record of gas apparatus in the world. Taking account of the results of the ultrasound velocity and the volume measurement, new empirical formulae for the pressure dependence of ultrasound velocities of helium, neon, argon, krypton and xenon were proposed. In addition, the volume and the sound velocity change of the krypton and helium gas mixture under high pressure up to 1.6 GPa were precisely measured with a high accuracy and a reliable concentration-pressure diagram is completed.

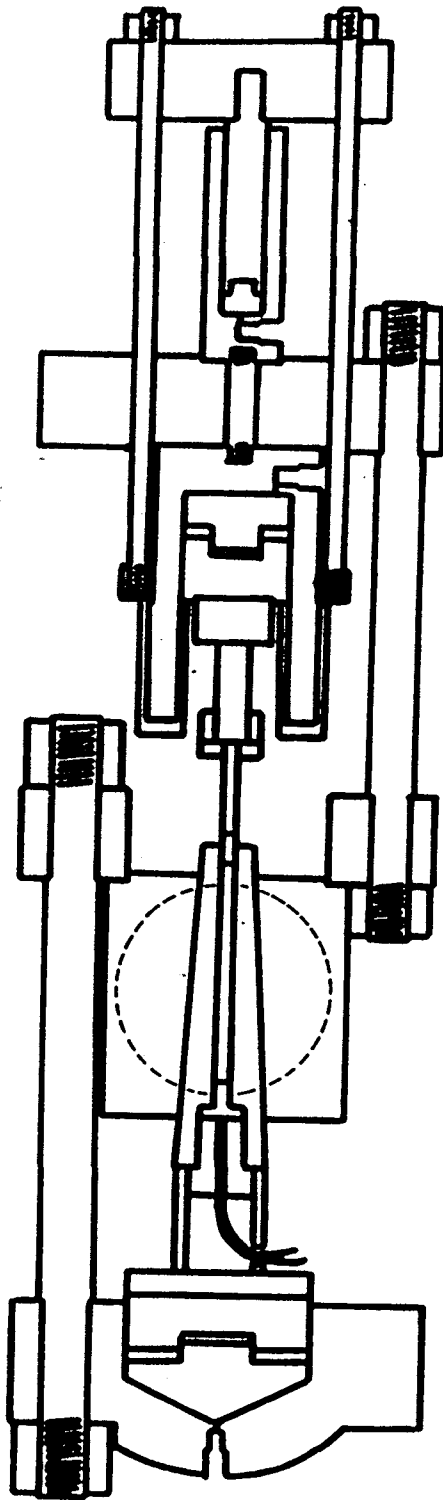


Fig. 1 Bridgman's piston cylinder apparatus.<sup>6)</sup>

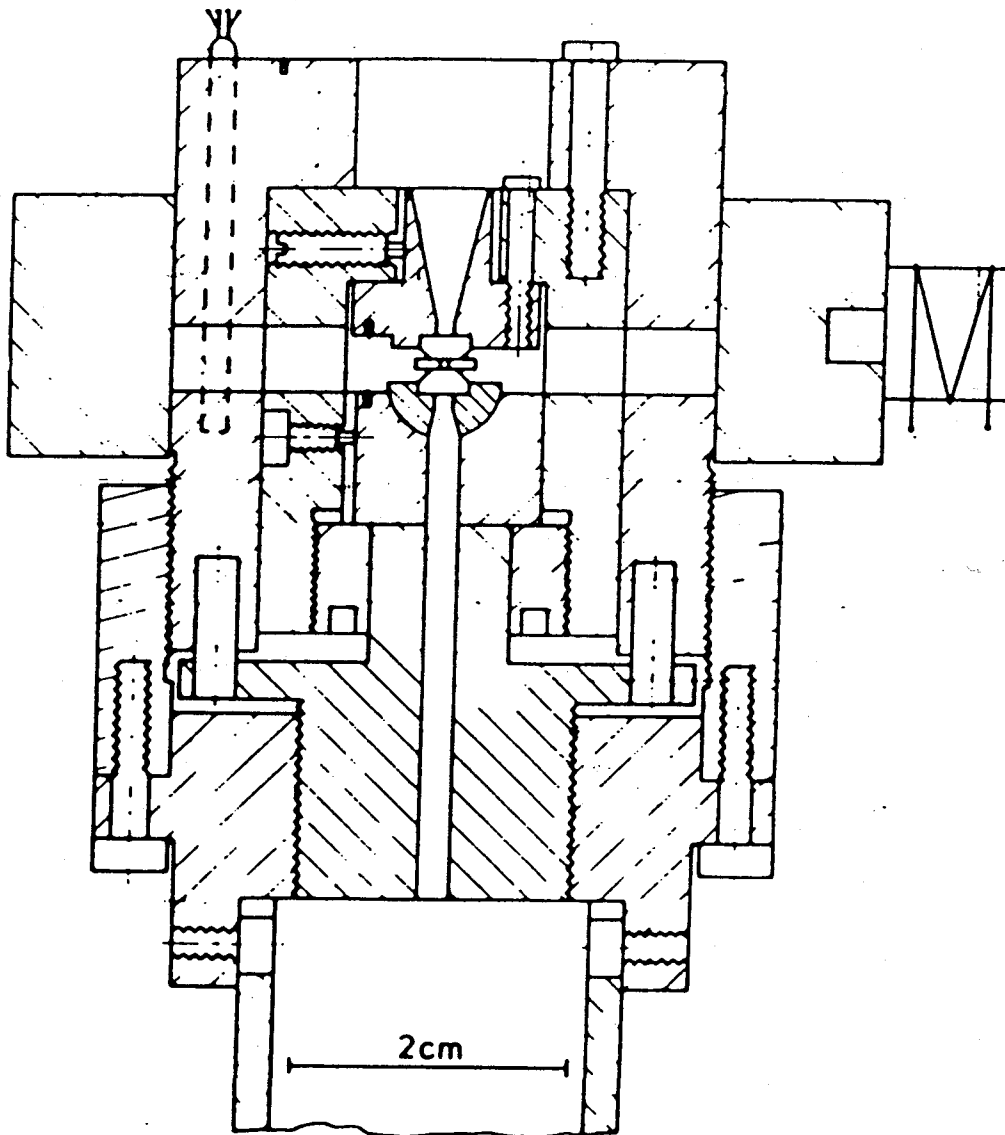


Fig. 2 Diamond anvil apparatus.<sup>20)</sup>

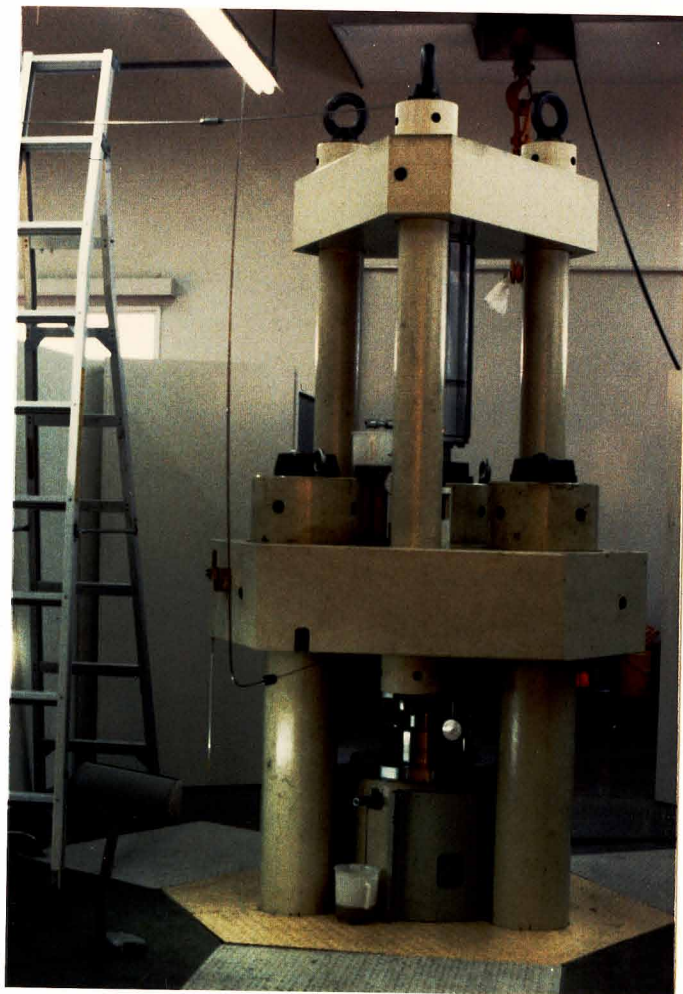


Photo. 1 High pressure gas apparatus.



## §2. Apparatus

### 2.1 Technique and main apparatus

The apparatus was intended to use neon or helium gas as the medium for transmitting pressure, because many other gases freeze below 3 GPa at room temperature. The procedure of the experiment is rather simple: Neon (helium) gas is compressed primarily up to 400 MPa, and introduced through a gas inlet tube to a high-pressure tapered cylinder in the main apparatus. Then, it is further compressed by a piston up to 4 GPa. The main apparatus is shown in Fig. 3. The frame of the apparatus comprises of three plates made of special forgings of steel and six tie rods made of JIS S45C steel. The upper and lower rams were made of DM steel of Hitachi Metals Ltd. with a hardness of Rockwell C 35.

The general principle of the design of the main apparatus was exactly the same as those<sup>36-38)</sup> originated by Bridgman.<sup>1)</sup> The gas pressure in the interior of the tapered cylinder is counterbalanced in part by pressure on the external surface which has the shape of a cone and is forced into the support ring by the lower ram with a capacity of 1200 tons (Fig. 3). The upper ram drives the piston with a capacity of 300 tons and a stroke of 300 mm, respectively. The packing of two rams were made of O-ring and three tapered rings, respectively. The total height of the main apparatus is almost 3.6 m.

### 2.2 High-pressure tapered cylinder

The main failure of the high-pressure gas apparatuses in the past, usually took the form of breaks in the cylinders. In the present apparatus, we used 350 maraging steel, which was

introduced by Lavergne and Whalley.<sup>41)</sup> The cylinder had a bore of 19.05 mm and the outer diameter was 130 mm at the base. The taper of the outer surface was 1/12. The cylinder was 262 mm long, and was heat-treated to a hardness of about Rockwell C 61.

There has been no problem, thus far, with respect to the cylinder fabricated in the above way, such as breaks, enlargement of the bore, and surface cracks. After more than ten exposures to pressures above 3 GPa, the diameters of the bore increased by less than 0.1 mm. Owing to the large value of the ratio of the outer and inner diameter (the wall ratio), of the cylinder in the present apparatus, 6, there had been no leakage with this amount of enlargement of the bore. It is safe to say that these cylinders could be used almost indefinitely without changing the dimensions of the seal packings.

### 2.3 Support ring

The support ring was machined from 300 maraging steel and 420 mm in diameter, and was 180 mm in length. After being heat-treated to Rockwell C 53-55, the flat surface and inner conical hole were finished by grinding. Then the ring was stretched by forcing a conical mandrel into the conical hole, up to a surface pressure of about 1.8 GPa. For this process the surfaces in contact were lubricated with 0.1 mm lead foil and Molykote G. The total stretch of the inner hole was unusually small and after six runs the permanent deformations was 0.3 percent of the original diameter. After stretched by the mandrel, the inner wall of the support ring was subjected to precision grinding; finally, the hole had diameters of 127 mm at the bottom and 112 mm at the top.

the tapers being 1/12 and 1/10 at the middle and bottom, respectively. To avoid dangerous rupture, the support ring was surrounded with a mild steel ring, so that the actual diameter of the support ring assembly was 500 mm.

No trouble has been encountered with respect to the support ring. After more than ten exposures to pressures above 3 GPa, the permanent elongation of the diameter of the hole was not more than 0.01 mm.

#### 2.4 Piston and packings

In Figs. 4 and 5, the high pressure piston and piston packings are shown, respectively. The high pressure piston is shown in Photo. 2. The piston was made of tungsten carbide D2 of Sumitomo Electric Industries Ltd. with compressive strength of 5.4 GPa. The piston had a diameter of 18.7 mm and a straight part of 125 mm so as to give a clearance of 0.35 mm and working distance of about 100 mm, respectively. Reduction of the working volume in the tapered cylinder to produce high pressure was done by the upper hydraulic ram piston actuated by oil with pneumatic pump.

For the piston packing assembly, which consisted of three hard parts and soft ring packings, we first employed the same sizes and materials as those used in previous experiments by another machine.<sup>38,39)</sup> They worked fairly well but permanent deformations remained in the hard steel parts. Therefore, they were replaced with new ones made of tungsten-carbide; since then, there have been no problems with the packing assembly. The new packings are shown in Photo. 3.

Except the neoprene ring, Teflon ring and other back-up rings, the assembly could be used almost indefinitely under pressures up to 3.5 GPa.

## 2.5 Bottom closure and packings

The bottom closure had the function of sealing the lower end of the high-pressure tapered cylinder and of providing a pressure-tight, insulating electrical connection to external circuits. In the present experiment, we used the bottom closure with five holes for electrical connections. The copies of the parts<sup>38,39)</sup> previously used up to 2.5 GPa were not always usable, because large permanent deformations often took place leading to the gas leakage and even to breaks in the closure.

The bottom closure and packings were newly designed and made, a cross section of which is shown in Fig. 6. The body of the closure was made of high-speed steel, HAP 50, of Hitachi Metal Ltd, with a Rockwell hardness, C 68. Among the packing, the cone, through which the wires were conducted to the external circuits, was made of Bear Cat steel of Bethlehem Steel Co..

For the sake of preventing leakage at the bottom closure, the lowest steel ring shown in Fig. 6 was most important. After some trials, we finally used 300 maraging steel for that part. The bottom packings are shown in Photo. 4. The new bottom closure assembly has been free from trouble.

The electrical connections were made through hardened steel cones insulated by thin conical sleeve of Lava, fine-grained pyrophyllite. 0.5 mm diameter copper conduction wires were silver soldered carefully to the tip and bottom of the steel

cones. The wires attached to the conetips were free from stress. Five separate leads have been successfully introduced to the external electrical connections. All the small parts included in the packing are shown in Fig. 7. An arrangement found very convenient was the use of a miniature socket attached to the measuring device in the high-pressure cell, which was indexed to plug into prongs extending upward and connecting to the 0.5 mm wire from the conductors in the bottom closure, as Fig. 7 shows.

## 2.6 Preliminary gas system

Since the available gas pressure from a commercial gas vessel is below 15 MPa, which was not high enough for the present purpose, the gas was compressed with two intensifiers in the preliminary gas system (Fig. 8). The first intensifier was 65 mm in inner diameter with 400 mm stroke. It could compress gas up to 200 MPa. The second intensifier was 43 mm in inner diameter with a 520 mm stroke. It had a maximum pressure capacity of 400 MPa. These two intensifiers were actuated by oil with two pneumatic pumps, respectively. Pneumatic pumps and preliminary apparatus are shown in Photo. 5. These cylinders of the two intensifiers were made of JIS SNCM 439 steel. Both of their pistons were made of JIS SKS 3 steel. This apparatus was free from oil-contamination.

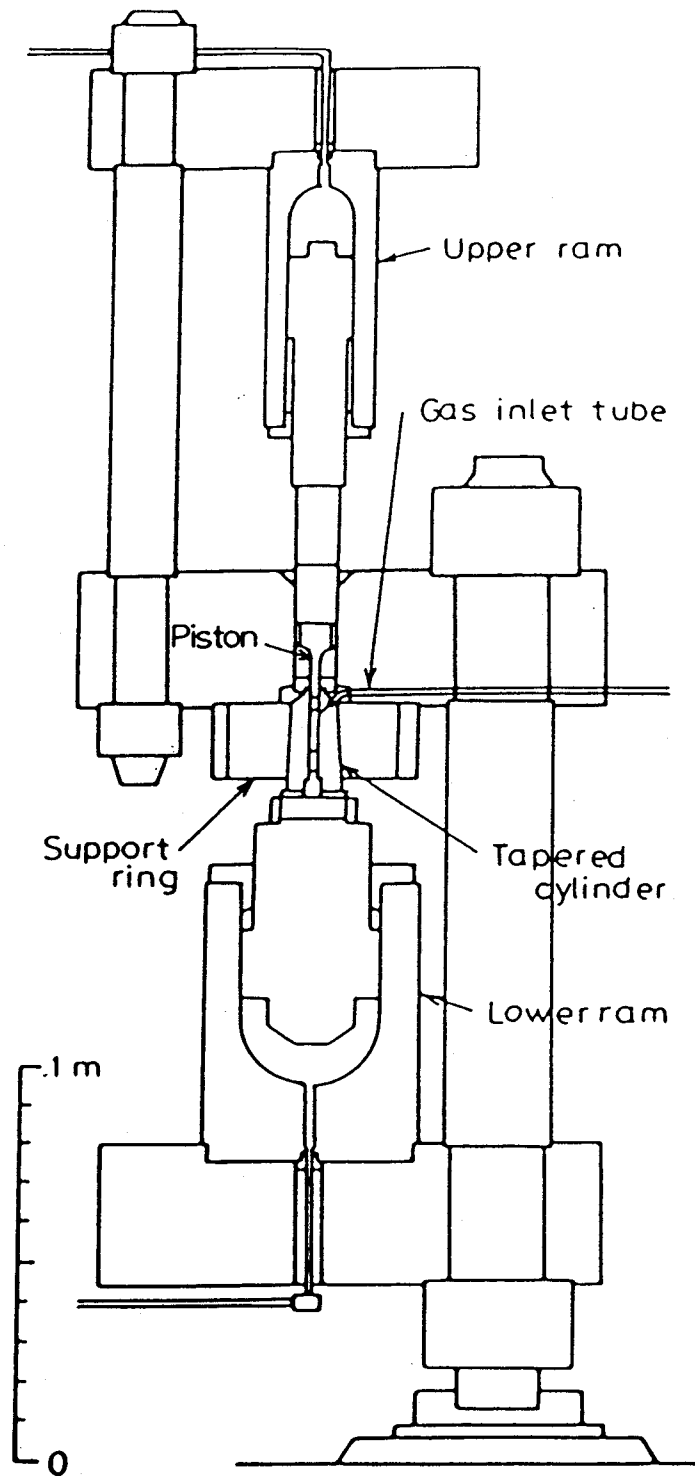


Fig. 3 Main apparatus.

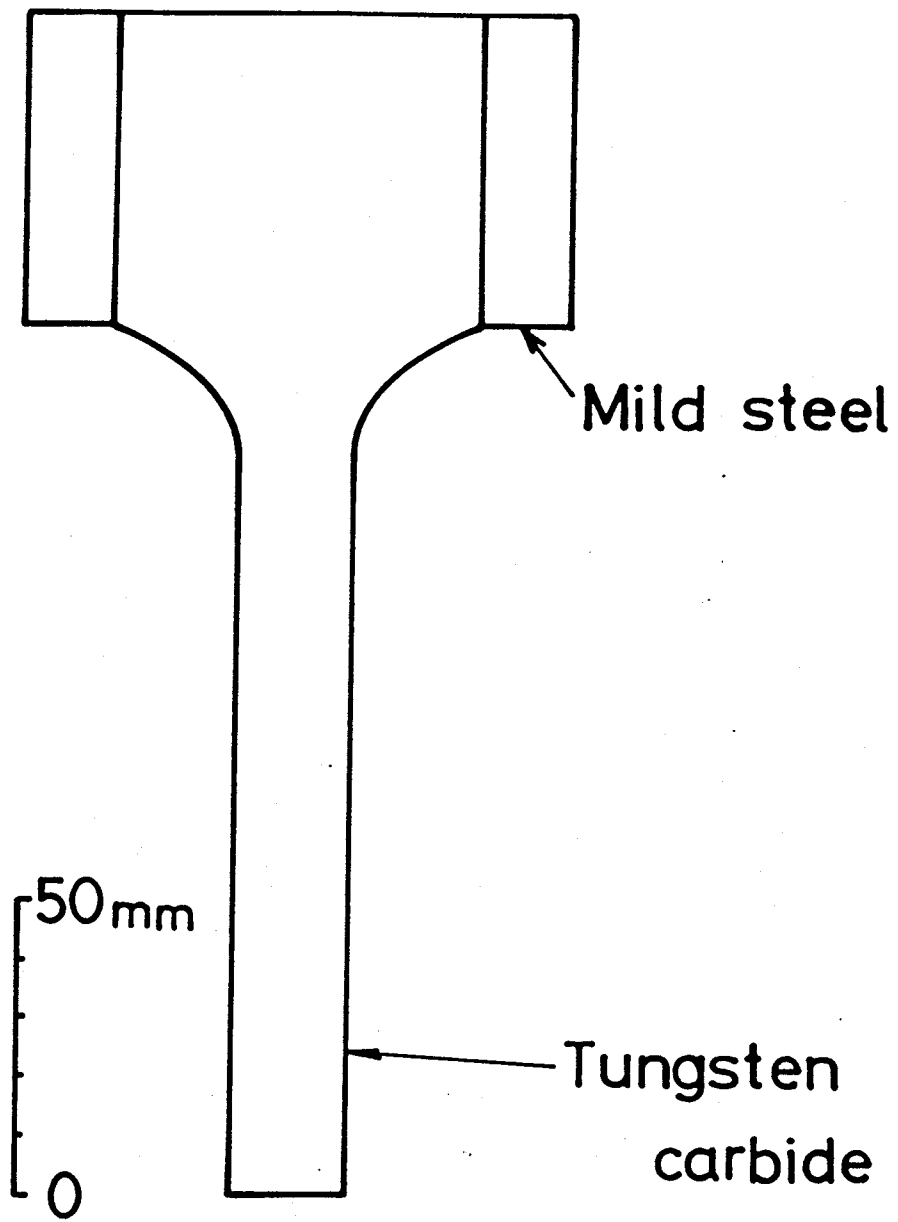


Fig. 4 High pressure piston.

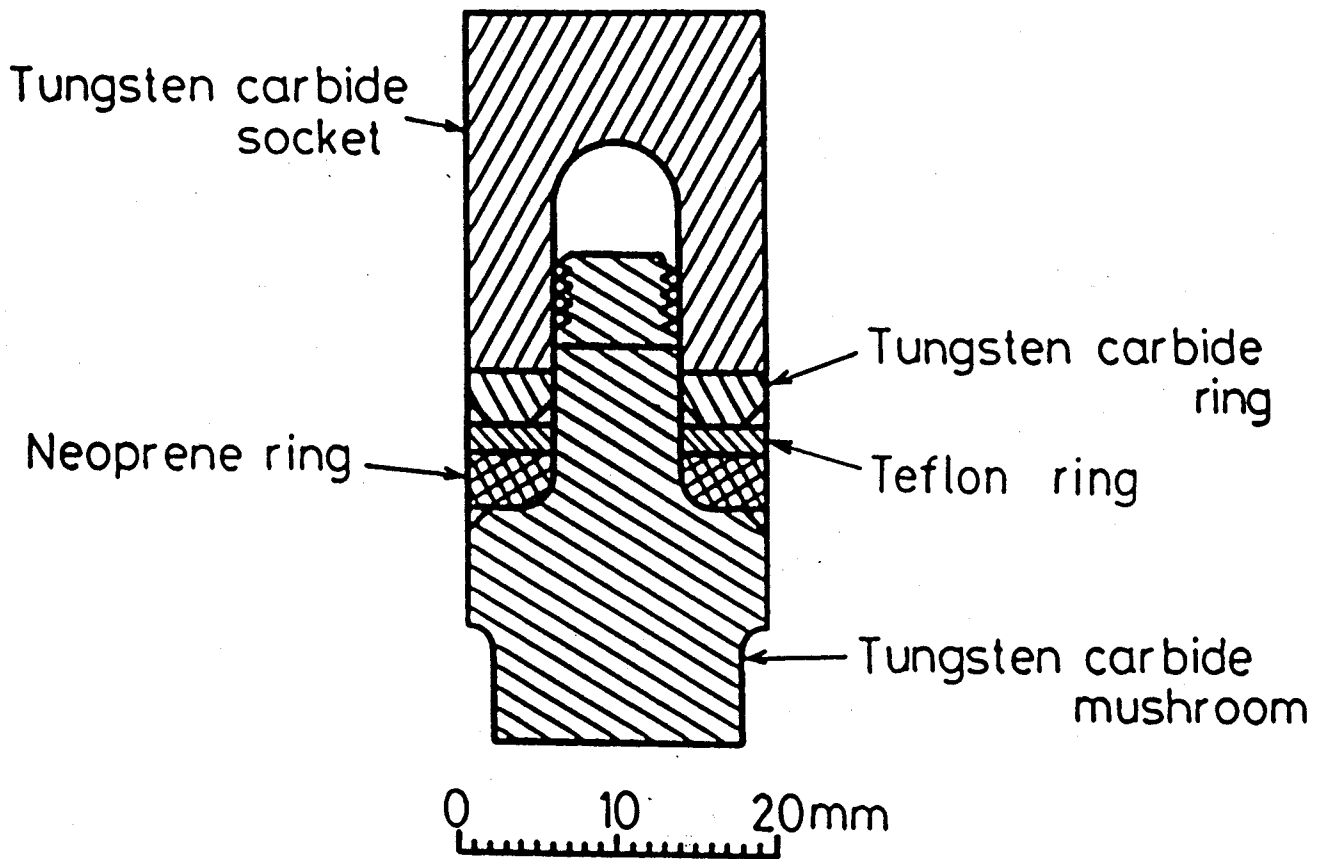


Fig. 5 Piston packings.



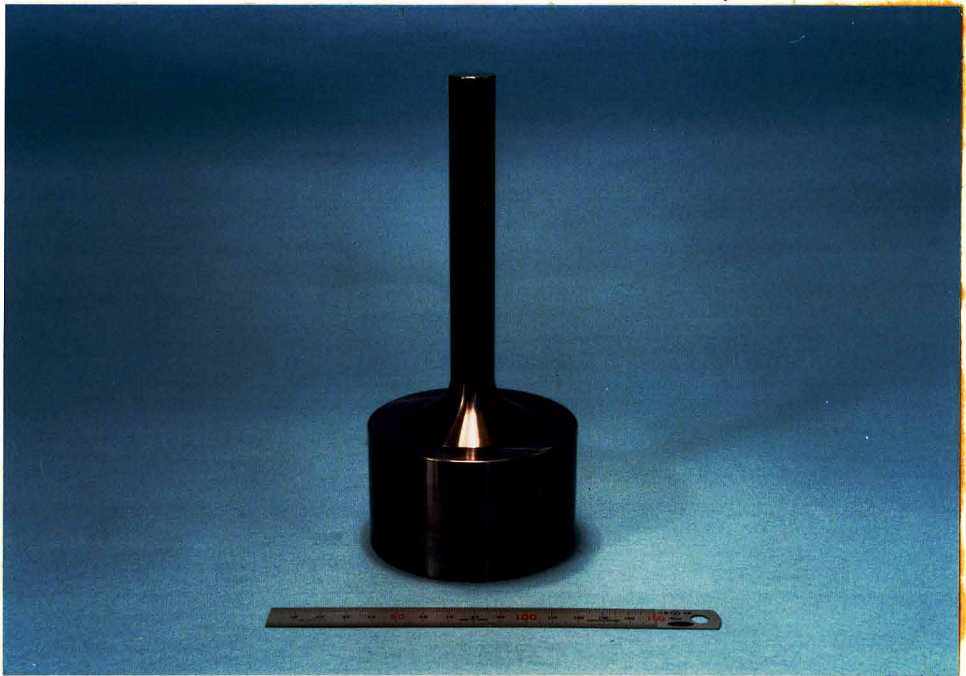


Photo. 2 Piston.

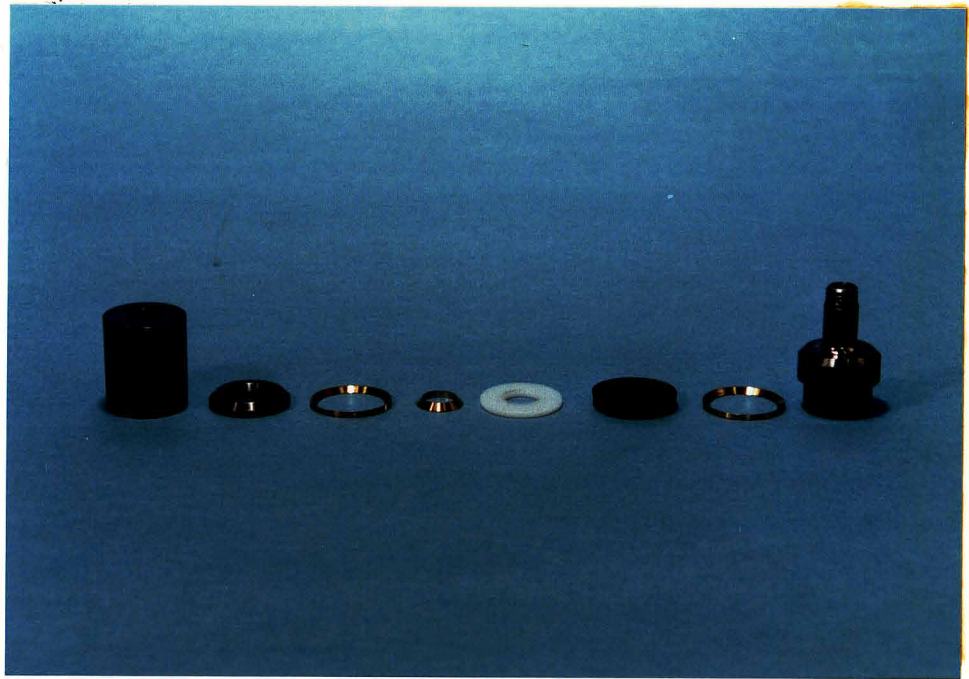


Photo. 3 Piston packings.

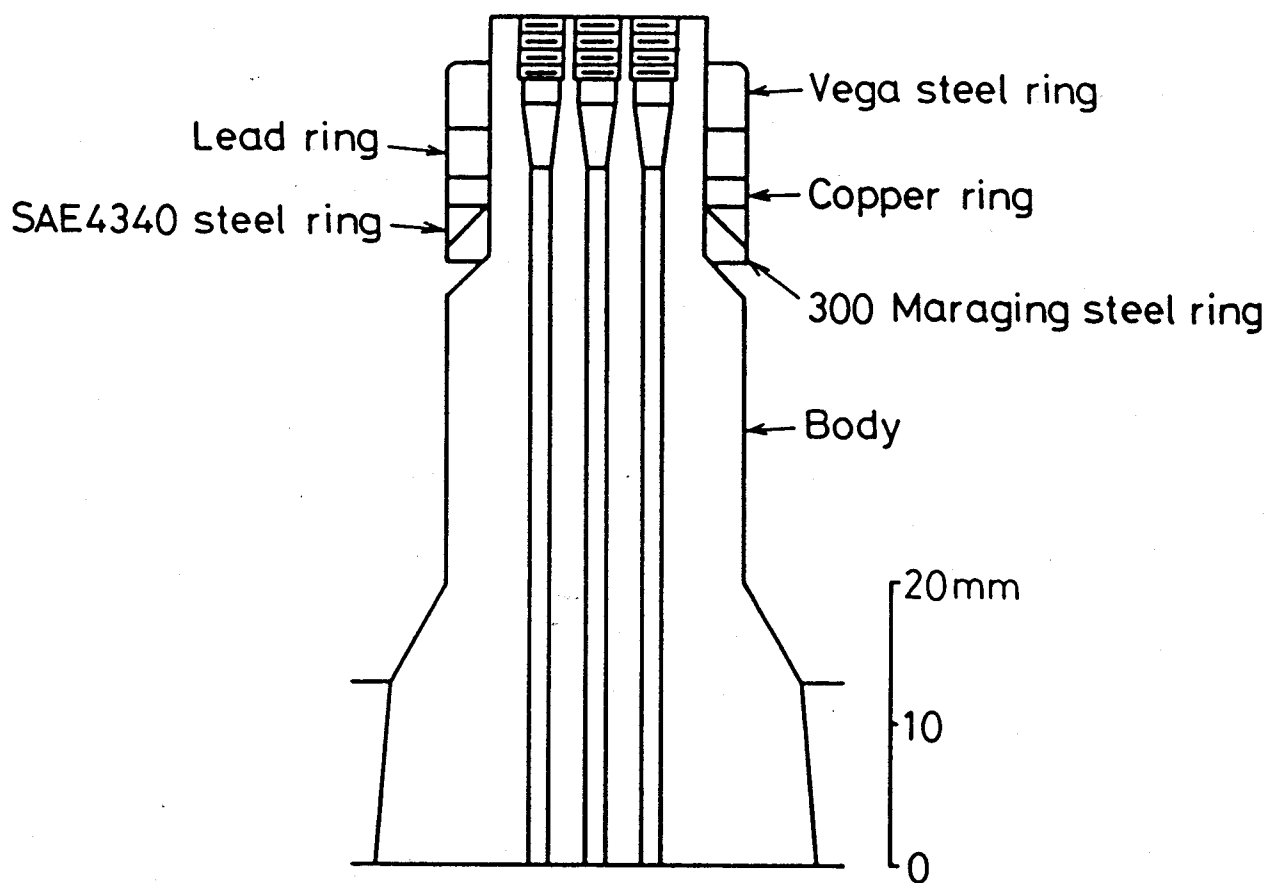


Fig. 6 Bottom closure and packings.

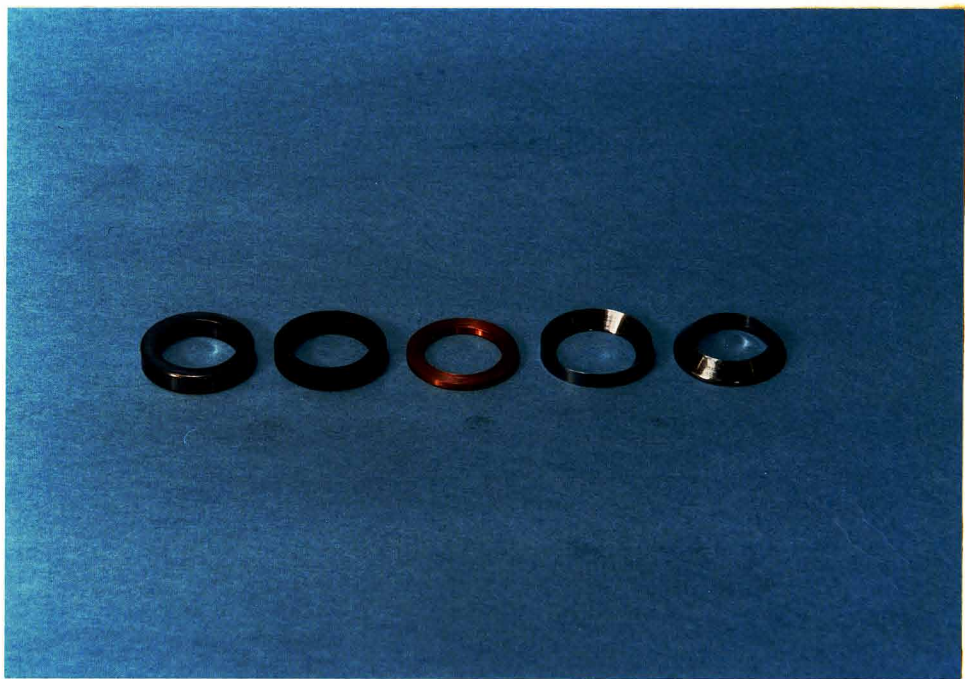


Photo. 4 Bottom packings.

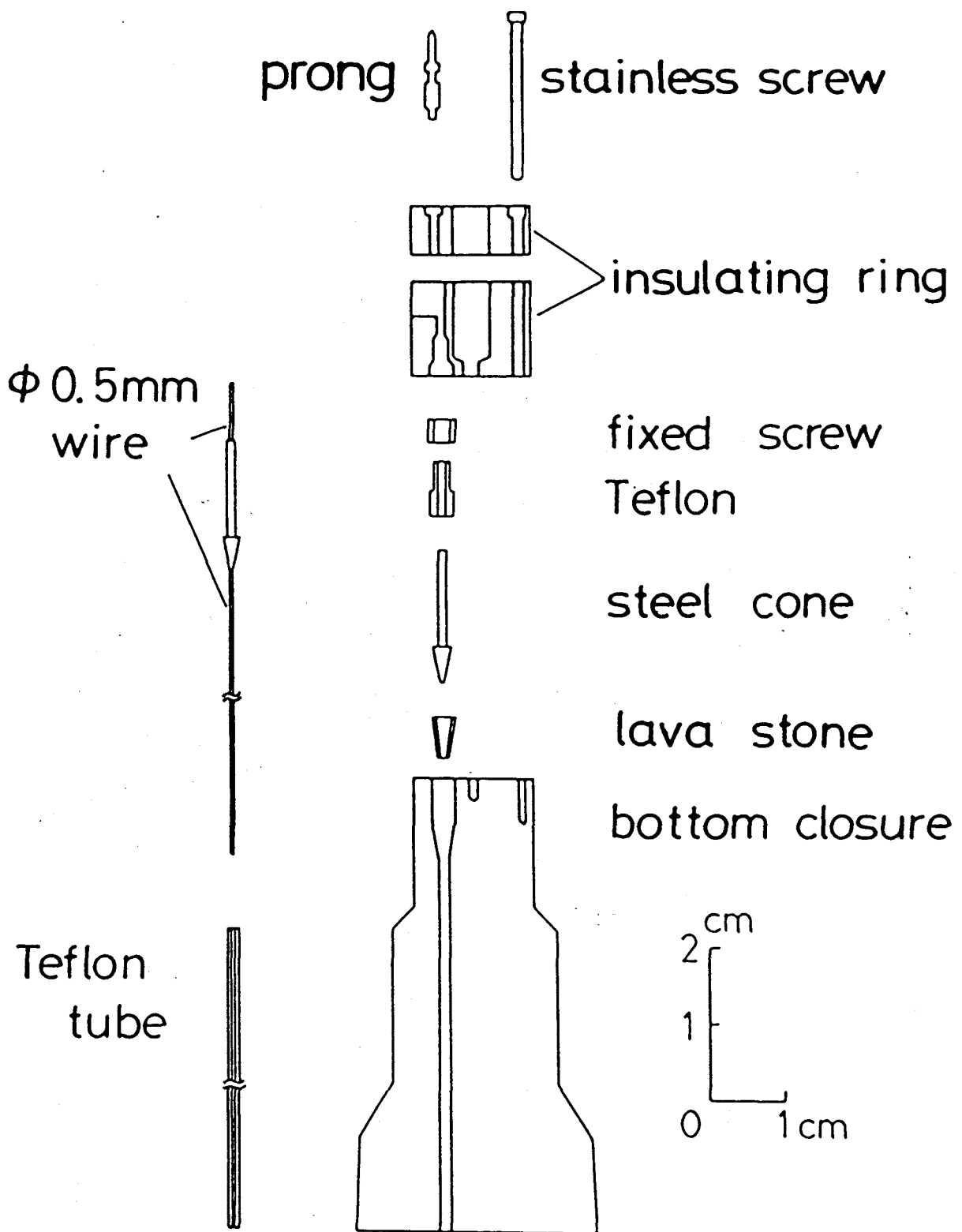


Fig. 7 Details of insulated conductors.

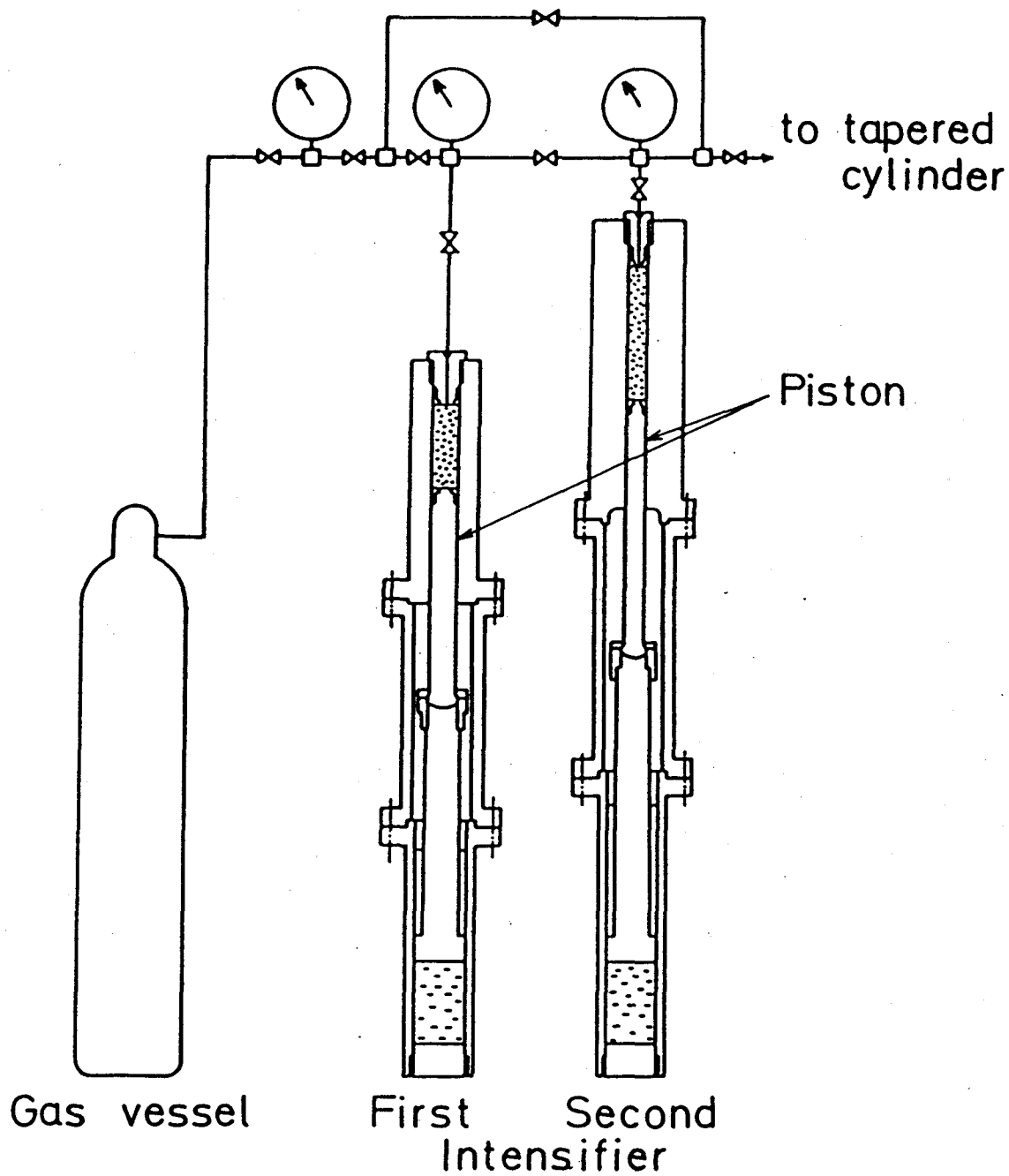


Fig. 8 Preliminary gas system.

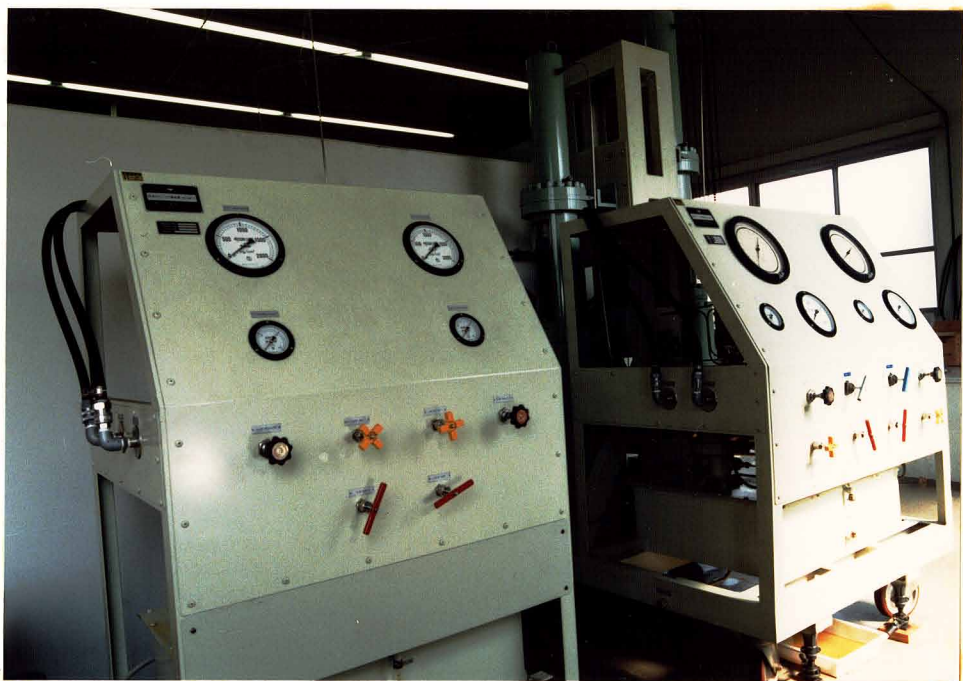


Photo. 5 Pneumatic pumps and preliminary apparatus.

## §3 Experimental procedure

### 3.1 Assembly of the pressure apparatus

The different parts of the press must be kept clean of foreign particles; therefore, before putting any two surfaces together they must be wiped clean.

The main apparatus, at the beginning of the run, had the bottom closure in place on the top of the lower ram piston.

For lubrication of the high-pressure tapered cylinder in the support ring three layers of materials were used. The inner layer next to the tapered cylinder was Molykote G. The second layer was 0.1 mm lead foil and covered tapered cylinder with no overlapping. The third layer was another one of Molykote G.

Before placing the tapered cylinder on the bottom closure the bottom packings must be put onto the bottom closure, as shown in Photo. 6. The tapered cylinder was placed on the bottom closure, as shown in Photo. 7. And the support ring was carefully placed on the high-pressure tapered cylinder. The sonic chamber was placed on the bottom closure with the electrical socket. The piston packings were inserted into the upper end of tapered cylinder. Then the gas inlet tube was connected to the high-pressure tapered cylinder. In order to place center, piston guide block was placed on the high-pressure tapered cylinder. The upper part of the main apparatus above the center plate was placed on the shoulders of the lower tie rods with a chain block. The three nuts on the lower tie rods were then screwed down by hand to the center plate.

The lower ram piston was pushed up, and the support ring was pressed to the bottom face of the center plate. The high-pressure



piston was placed on the piston packing. Two blocks were placed on the piston, and then the upper ram piston was started to press down these blocks.

After assembling the main apparatus completely, the air must be excluded from the high-pressure tapered cylinder. In order to do this, the high-pressure tapered cylinder was filled with the pressure medium gas above 10 MPa in pressure, which was kept for 5 minutes or so and discharged. After repeating this for seven times, the gas pressurized to 350 MPa with the preliminary gas apparatus was introduced in the cylinder. The pressure calibration was done by measuring the electrical resistance of a manganin wire adjusting the potentiometer before the bridge circuit.

### 3.2 Measurement of pressure

Five electrical wires through the bottom closure were used for a pressure gauge (manganin gauge), thermocouple, heater, and emitting-receiving pulses of ultrasound waves. In principle, all these measurements could be made simultaneously but in the present experiment only three out of the four circuits were used at one time in order to avoid noises from interferences.

Pressure was measured by a coil of manganin wire placed just above the bottom closure. Either of two manganin wires of resistance of 120 or 50 ohms, properly heat-treated and covered with silk, was used. The gauges were calibrated with the freezing point of mercury at 20.6 °C and 1.17 GPa given by Molinar, Bean, Houck and Welch.<sup>61)</sup> The change in the resistance of a manganin gauge under high pressure was converted to voltage and recorded with a multi-pen-recorder. The sensitivity of resistance

measurement corresponded to a pressure difference of 1 MPa.

The square term of resistance-variation under high pressure was taken from the mean value of the data by Peggs and Wiśniewski,<sup>62)</sup> and those by Ruoff, Lincoln and Chen,<sup>63)</sup> which was  $2 \times 10^{-10} P^2$ . The formula used to determine the pressure is

$$\frac{\Delta R}{R} = 2.3739 \times 10^{-5} P - 2 \times 10^{-10} P^2,$$

where R,  $\Delta R$  and P are the resistance, change of resistance and pressure in MPa, respectively.

### 3.3 Measurement of temperature

For a temperature measurement, a platinum-13 % rhodium wire was used, along with a platinum winding for heating. Furnace assembly is shown in Fig. 9. The details of furnace design were varied in efforts to prolong the life of windings, to improve temperature distribution, and facilitate loading and unloading. The body of the furnace with a bore of 6 mm, an outer diameter of 18 mm, and length of 40 mm was closed by two caps as shown in Fig. 10. A furnace winding with an outer diameter of 5.5 mm, bore of 3.5 mm and length of 28 mm with winding pitch of 1 mm was inserted in the furnace body. In the furnace winding were set three spacers and a platinum tube, in which a sample was placed. The heating wire of 0.2 mm in diameter was made of platinum too. The parts of this assembly were almost the same as those used in previous experiment,<sup>38)</sup> and no trouble has been encountered. In Fig. 11, electric circuit is shown. The multi-pen-recorder mentioned above was used also for recording temperature.

### 3.4 Measurement of ultrasound wave velocity

Two methods were possible for measuring the ultrasound wave velocity under high pressure. In the present experiment, however, the ultrasound velocity was determined only by the single-pulse method, which was less accurate but much easier than the other method of pulse-superposition.<sup>64)</sup> Actually, there was no need of calibration for the former, since an accuracy better than 0.2 percent was not required.

In Fig. 12 the sonic chambers are shown along with the manganin gauge. A spacer placed between two piezo-electric crystals in each chamber was a thin-walled cylinder of 8 mm in height made of cold rolled steel. Many holes in the wall (Fig. 13) were absolutely necessary in the mixed gas experiment, because when separation took place, the separated gases and liquids were required to move through the holes instantly. In the case of the measurement of a gas mixture, two sonic chambers of the same type (vertically arranged as in Fig. 12) were necessary.<sup>65)</sup>

The elastic constants of the spacer were measured by a single pulse method before the high-pressure run. The velocity  $U$  in a gas under pressure  $P$  was then given by the equations:

$$U = \frac{L}{t} \quad (1)$$

and

$$L = L_0 \left( 1 - \frac{K_0}{3} P \right), \quad (2)$$

where  $L_0$ ,  $L$ ,  $t$  and  $K_0$  are the length of the spacer at zero pressure, length of spacer at  $P$ , traveling time and compressibility of the spacer at zero pressure, respectively. The above equations neglect the pressure-dependency of the compressibility, but the correction for it was only about 0.05 percent.<sup>66)</sup>

Sonic chambers are shown in Photo. 8. The two sonic chambers were connected with coaxial cables and a steel spring, which kept the upper one always at the uppermost part of the cylinder and the lower one at the bottom. The latter was fixed to the bottom.

An electric socket attached to the lower sonic chamber made it possible to remove the two sonic chambers through the upper end of the cylinder without disturbing the bottom closure.

In each sonic chamber, a pair of lead zirconate titanate crystals with a 14 mm diameter and a fundamental frequency of 1 or 2 MHz were set at the ends of the before mentioned spacer and acted as driver and receiver, respectively. Devices of measurement of ultrasound wave velocity are shown in Photo. 9. The pulse generator used was a Hewlett Packard model 214A and was triggered from outside by a signal generator of Anritsu Electric Co. MG417A. The out-put electric pulse with 5 ns rise time from the pulse generator was introduced to a piezo-electric crystal in the high pressure cylinder. The pulse from the detecting crystal was displayed on Iwatsu SS-5500 and SS-5302 oscilloscopes together with a time mark generator Tektronix type 181. The displayed pulses were photographed and measured with a comparator of Mikuni Maching Co. origins No.2 with an accuracy of 0.001 mm. The above method was used for the single-pulse-measurements in

the high pressure experiment. For calibration a pulse superposition method was used, with a frequency counter Iwatsu Electric Co. UC-8151. Throughout the present experiment, the accuracy of the velocity-measurement was within 0.2 percent.

### 3.5 Measurement of Volume

One of the most difficult measurements under high pressure is the volume of a gas. In the present experiments, volume measurements were achieved by using almost the same method as mentioned by Bridgman.<sup>1)</sup> The piston advanced into the cylinder up to 100 mm, and the travel-distances were measured from outside by an electric micrometer within an accuracy of 0.0005 mm. The vertical distortions of both the piston and bottom closure were estimated from the elastic moduli of the constituent materials.

As to the radial distortion of the cylinder by gas apparatus, the radial displacements were calculated using the theory of elasticity on multi-cylinders with non-uniform stress distribution.

An absolute measurement of the volume was not made in the experiments and, hence, the standard values of volumes of gases were taken from the data by other investigators cited in each case in §5.

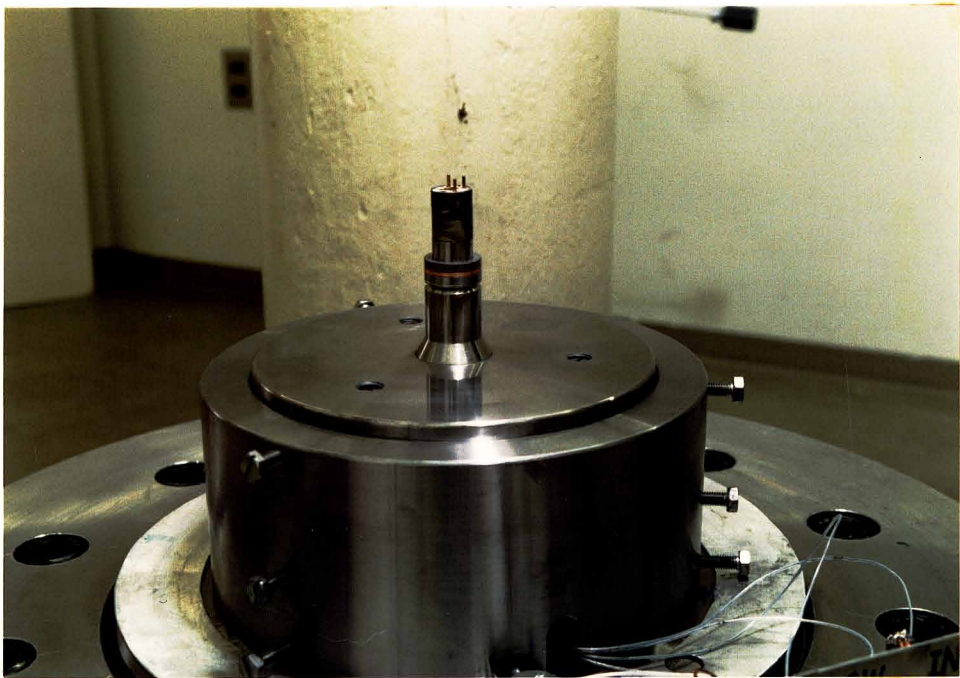


Photo. 6 Assembly of bottom closure with bottom packings.

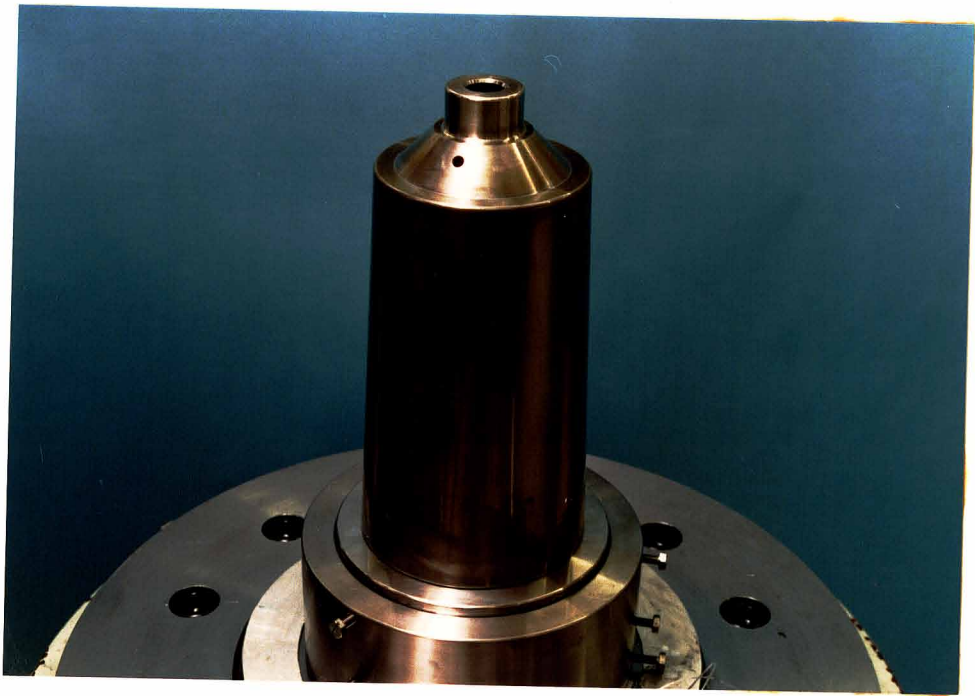


Photo. 7 High pressure cylinder set on the bottom closure.

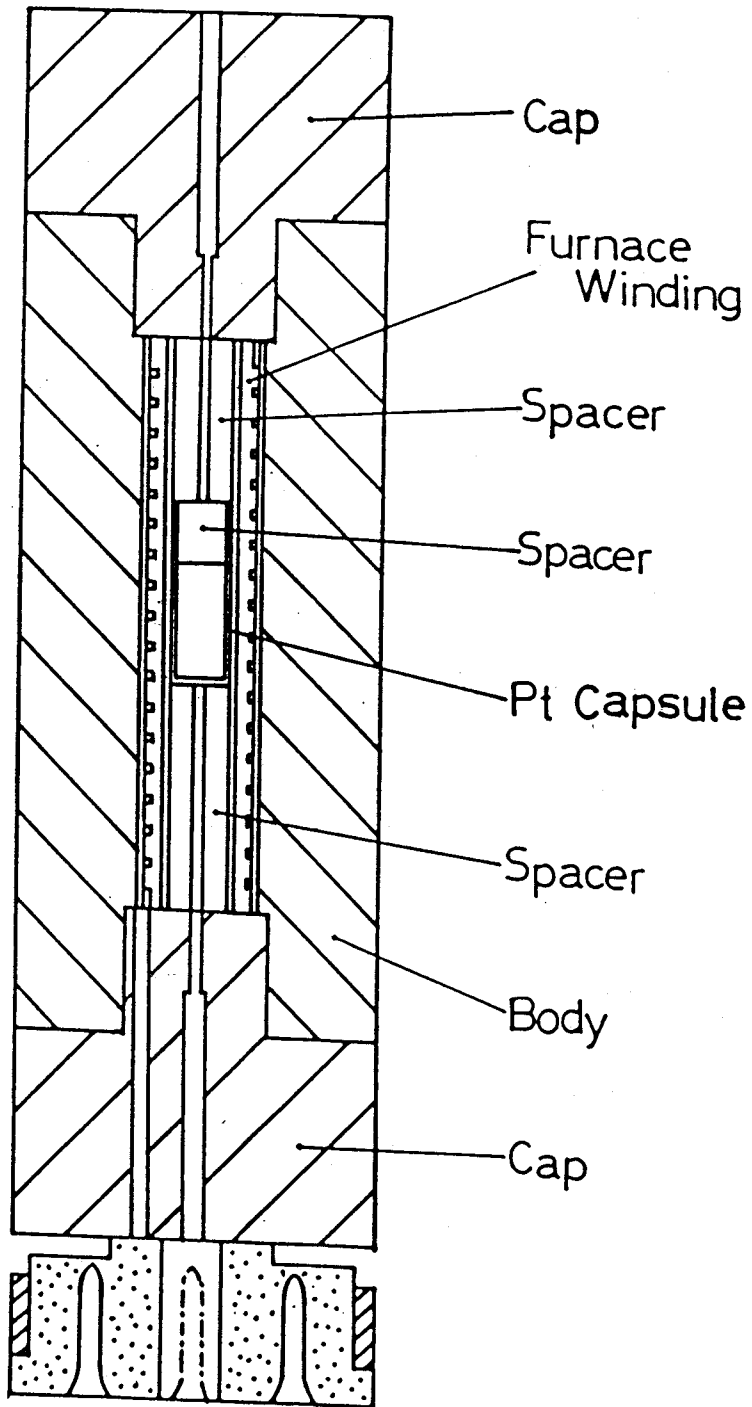


Fig. 9 Furnace.



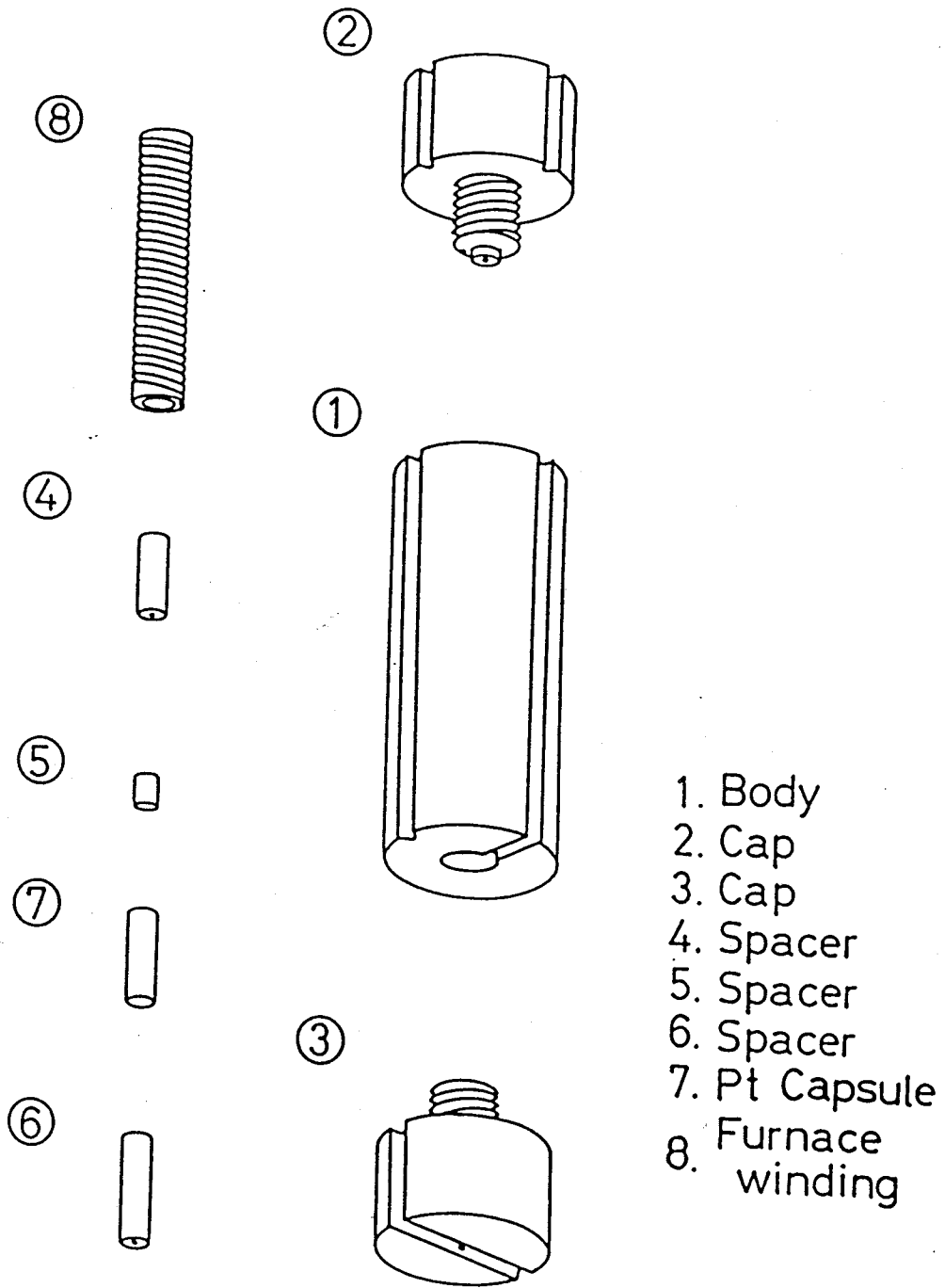


Fig. 10 Furnace parts.

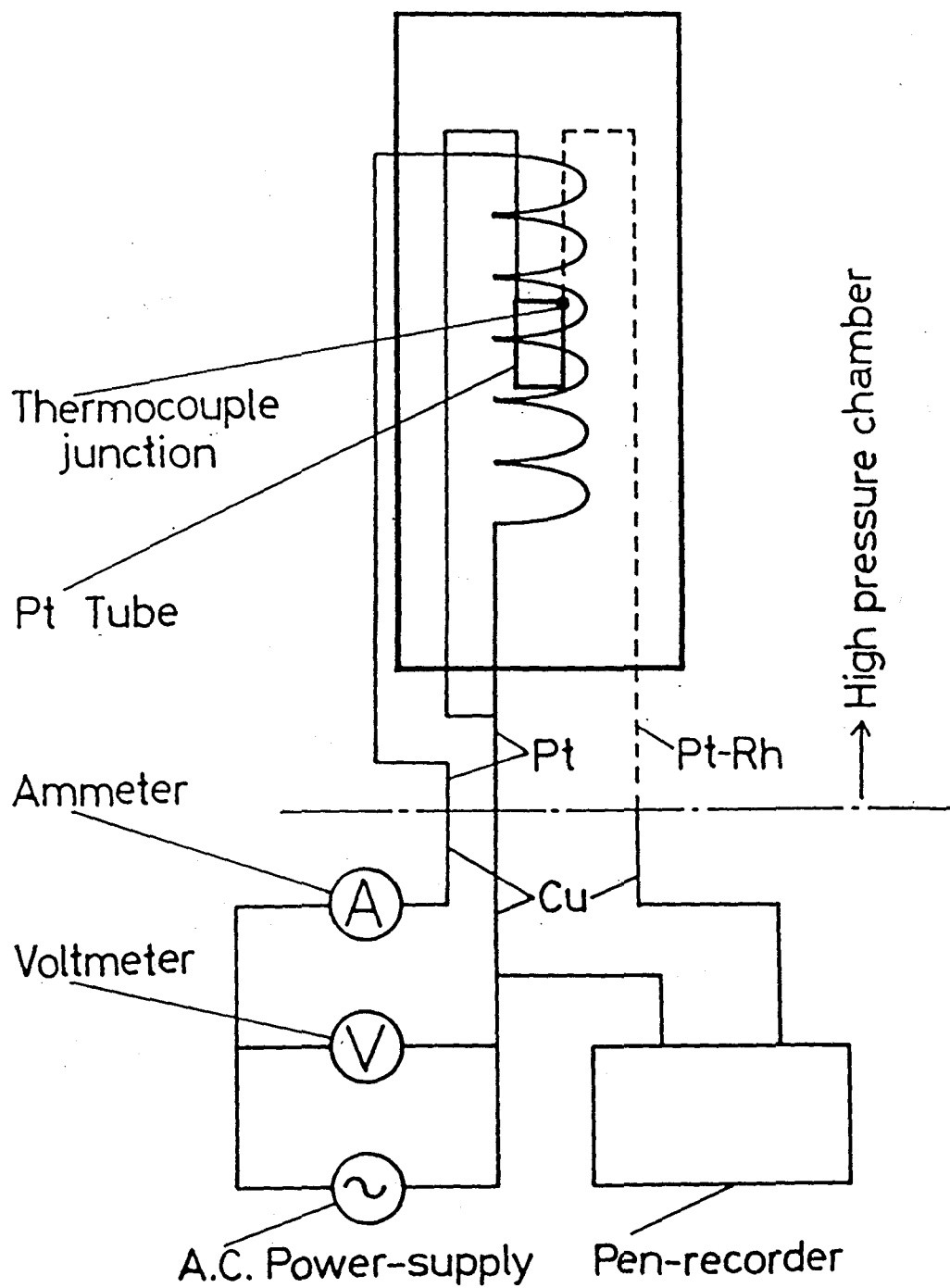


Fig. 11 Electric circuit of furnace .

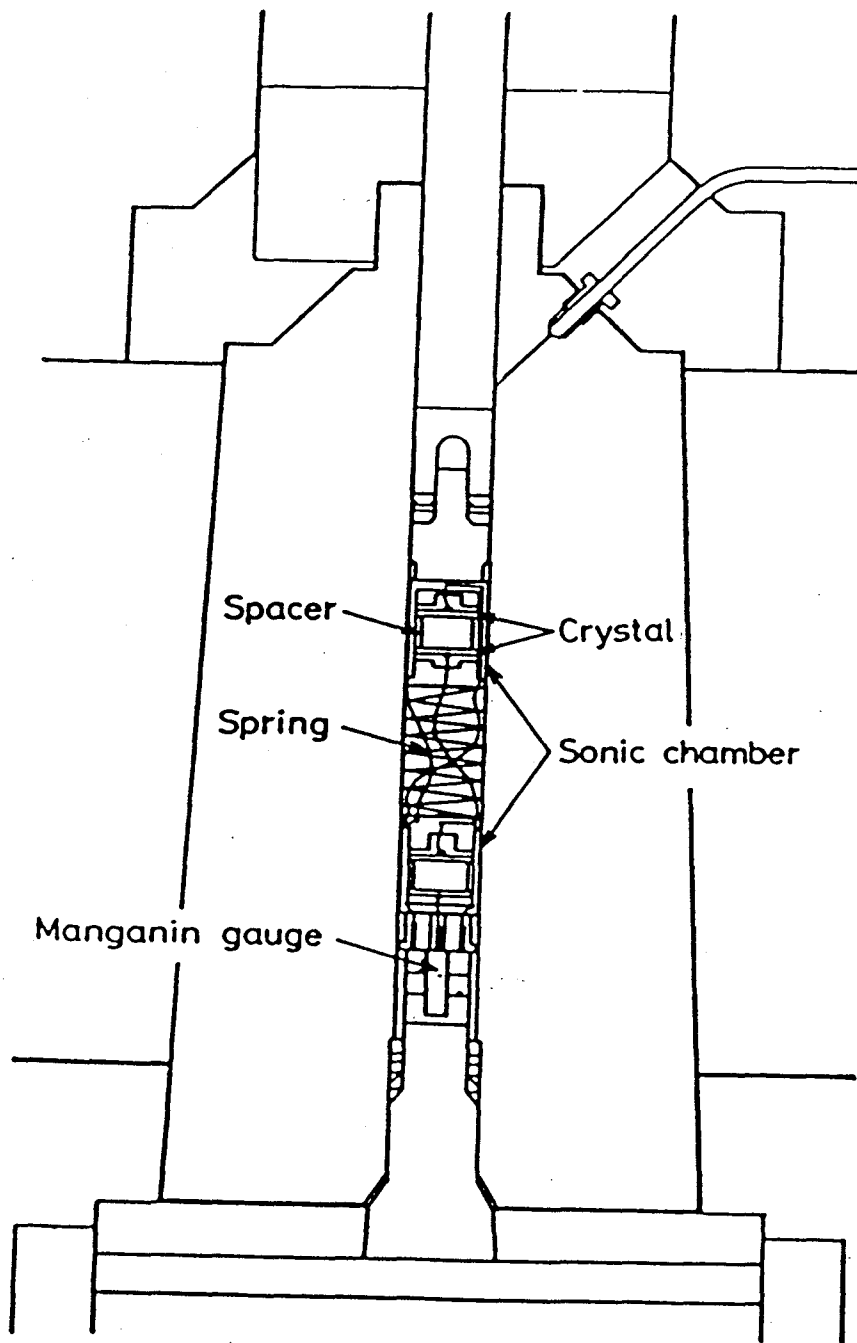


Fig. 12 Sonic chambers in the cylinder.

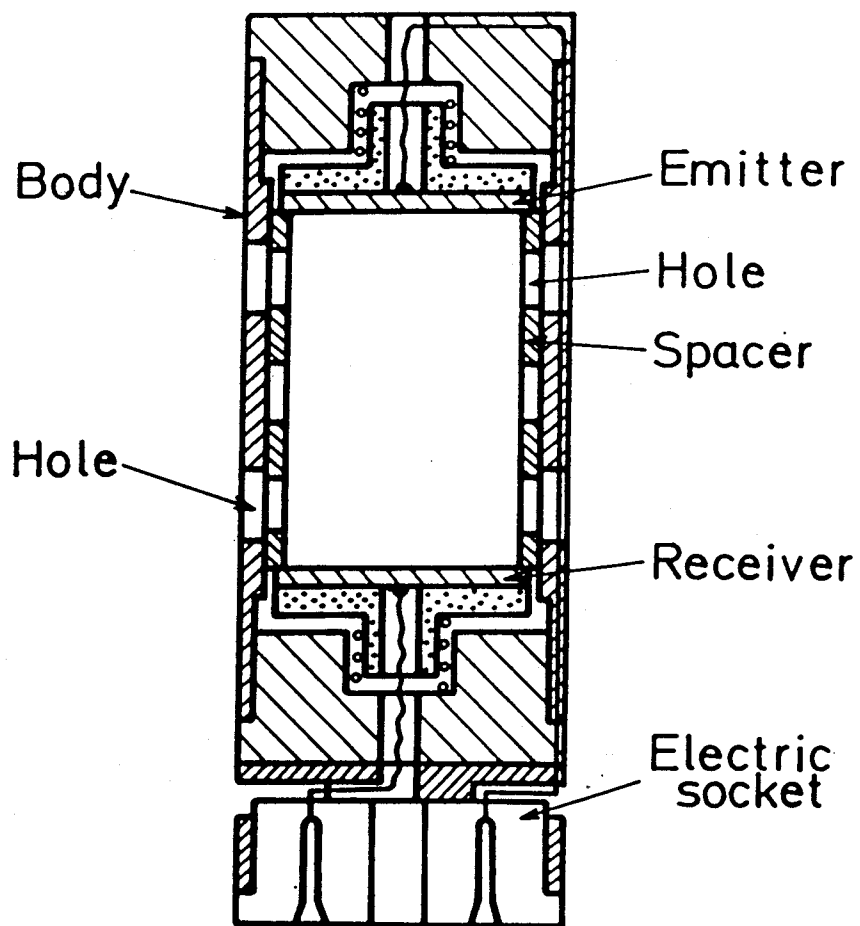


Fig. 13 Sonic chamber.

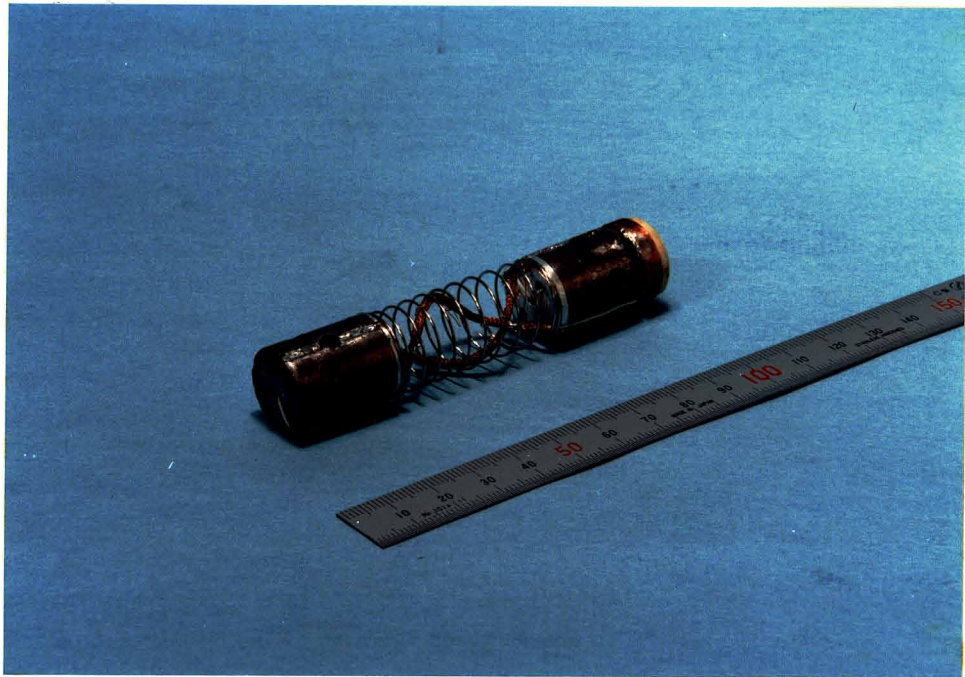


Photo. 8 Sonic chambers.

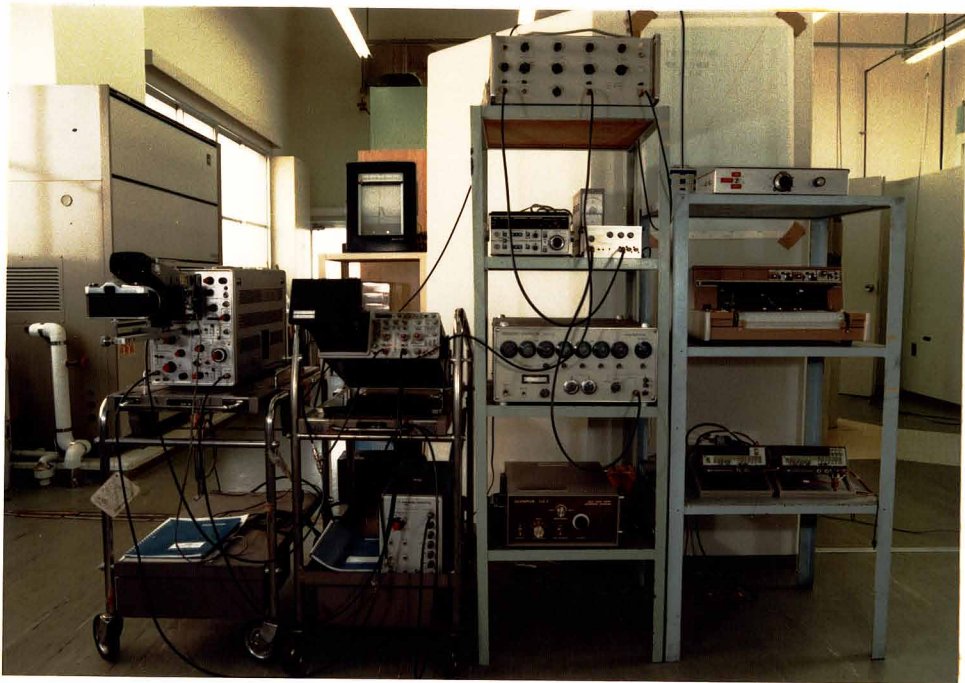


Photo. 9 Devices of measurement of ultrasound wave.

## §4. Measurement of Freezing Point and Phase-Separation

### 4.1 Detection of freezing point

The velocity of ultrasound waves increases smoothly with pressure; however, at the freezing point it is usually observed that the velocity increases suddenly.

To determine the freezing point of gases, the simplest way is to detect a discontinuous change of velocity with respect to a pressure change. There are also other ways to detect the freezing point, such as measurements of both the piston movement and the pressure. The above three methods have frequently been used recently by many investigators.<sup>6, 44, 49-51, 67-69</sup> In the case of the gas mixture, the above methods are still valid.

There appeared not only one abrupt change in the measured velocity during one high-pressure run. In the transition of the gas-solid type, the abrupt change in the velocity was always associated with a change of amplitude and wave form of the acoustic pulse, probably because of precipitation of solids on the piezo-electric crystals. In the transition of gas-gas separation, no abrupt change in the amplitude and the wave form (but only that of the velocity) was observed.

Throughout this study, the detection of the freezing point in a mixture of gases was always assured by a discontinuous change in the velocity accompanied by an abrupt change in the amplitude and the wave form of the acoustic pulse. There was no confusion, therefore, between gas-gas separation and solidification in the analysis.

## 4.2 Detection of phase separation

Let us consider a homogeneous binary mixture of gases at low pressures, which separates into two gas phases when pressurized, and then solidifies under higher pressure, as shown by a diagram of Fig. 14(a). When separation starts, a new phase with a high concentration of a heavy gas, which is represented by a point E in the figure, appears. The domain BCDE in Fig. 14(a) represents the region of the co-existence of the two gas phases; above CD the heavy gas phase re-separates into a solid state H and a gas state C. At the pressure of CDH, three phases, gas C, gas D and solid H, coexist. Suppose that the velocity of ultrasound waves in the pressurized gas is measured by using two small sonic chambers located at the top and bottom part of the pressure vessel (already described in the preceding paper). Since the light gas will rise to the top chamber and the heavy gas will fall to the bottom chamber, the measured velocities will be different between the two chambers, as schematically shown in Fig. 14(b).

By increasing the gas pressure from A in Fig. 14(a), a phase separation will take place at B; then the separated light and heavy gases will change their concentrations along lines BC, and ED, respectively. The reaction rates in the binary gas system are so fast that one can detect the change of the ultrasound velocities at the two sonic chambers as soon as the phase separation and freezing start. The expected pressure dependence of the velocities of ultrasound waves at the top and bottom sonic chambers are given by the upper and the lower branches of the curve in Fig. 14(b). Line A'B'C'F' indicates the velocity



measured at the top chamber, and line A'B'E'D'G' that at the bottom chamber, respectively. The discontinuity at B'E' for the bottom chamber is due to the gas-gas separation associated with a discontinuous concentration change from B to E in Fig. 14(a). Another discontinuity at D' in Fig. 14(b) arises from the solidification of the heavy gas at D in Fig. 14(a). The above description is exact only if the sonic chambers are very small.

In actual experiments, the above characteristic changes are slightly modified and diffused. An example of the velocity measurement in the present experiment for a 15 percent krypton and 85 percent helium mixture is shown in Fig. 15. No differences between the velocities in the upper and lower sonic chambers were found from  $A_0$  to a point slightly above  $B_0$ . Above  $B_0$ , the velocity obtained from the upper sonic chamber changed along  $B_0C_0F_0$  and that from the lower one along  $B_0E_0D_0G_0$ . There appeared discontinuities at around  $B_0$  and at  $D_0$ .

The coincidence of the two velocities from  $A_0$  to  $B_0$  was natural owing to the homogeneous phase of the gas. The coincidence in excess up to a point slightly above  $B_0$  was entirely due to the effect of the lower chamber's size. At  $B_0$  in Fig. 15, the heavier gas appeared and settled down first somewhere around the packings in the bottom closure of the high-pressure cylinder. At this moment, the lighter, newly separated gas still filled both the upper and lower sonic chambers. As the pressure was increased the amount of the heavier gas increased, reaching the lower chamber; finally, at  $E_0$ , the lower chamber was completely filled with the heavier gas. Above  $E_0$ , the ultrasound velocity in the lighter gas was measured in the upper sonic

chamber, and that in the heavier gas in the lower chamber, respectively. At  $D_0$ , the gases solidified at the lower sonic chamber, and so the velocity increased almost discontinuously to  $G_0$ , in Fig. 15.

From Fig. 15, it was very easy to determine the pressures of the transitions of both the gas-gas and gas-solid phases. For the gas-gas separation, the data at the upper sonic chamber showed the transition point indicated as  $B_0$  in Fig. 15. In this case the velocities at the upper sonic chamber did not change discontinuously, because the concentration of the lighter gas changed continuously. However, the transition point could be clearly detected by a change of the slope at  $B_0$  (Fig. 15). For the gas-solid transition, the data at the lower sonic chamber showed the abrupt change of the velocity as indicated by  $D_0$  in Fig. 15, since the precipitated solids piled up on the piezo-electric crystals in the lower chamber as mentioned before.

Thus, we could obtain the transition pressure ( $B_0$ ) of gas-gas separation from the upper sonic chamber, and the univariant pressure  $P_3$  of three phases ( $D_0$ ) from the lower one for the mixtures of 8~20 percent krypton. On the other hand, for the gas mixtures of 30~60 percent krypton, both the gas-gas phase separation and the solid condensation could be detected at the lower sonic chamber. In the use of the two chambers, there was no essential problem with their finite sizes to detect the pressures of the transitions.

There was another kind of phase separation which occurred in the case of more than 70 percent krypton-content; the gas-mixture separated first into a solid and a gas phase, and then at the

higher univariant pressure  $P_3$ , where three phases were in equilibrium, the gas phase solidified again. In this case, at the upper chamber we could detect both the solidification and the univariant pressure. The changes were easily recognized owing to the precipitation of solids, and entirely independent of the size of the upper chamber.

It is worth mentioning the time necessary to obtain an equilibrium in the phase transitions. It depended mainly on the design of the spacer mentioned in §3, and partially on the designs and arrangements of other parts inside the high-pressure cylinder. The spacer had many holes in its wall through which gases could instantly move and separate to reach the equilibrium.

During a few runs, the changes of the ultrasound wave velocities with the lapse of time after compression of the gases were measured as Fig. 16 shows. In all cases, the velocities became a constant value about two minutes after the compression, and during the following several hours no changes were observed. The gas-gas separation seemed to reach completion within a few minutes by the aid of gravitation and the free movement of gases through the holes of the spacer.

On the contrary, the reverse process from the separate gases to a homogeneous gas was very sluggish and the process could not be observed even in a three-days-measurement.

Regarding the gas-solid separation, though more than a dozen measurements were made, phenomena corresponding to super-cooling or over-heating were not observed.

It was found that reactions from gas to solid and vice versa were rapid in both compression and decompression and were

completed in a few minutes. Therefore, in the present experiment all measurements were made for about five minutes after the pressure was raised or reduced. Hanayama<sup>70)</sup> had already used the same technique in the study of a xenon-helium mixture, and confirmed the rapid reactions of gases under high pressure.

In conclusion, the pressures of the transitions from gas to gas or to solid could be exactly measured by using two sonic chambers placed in the upper and the lower part of the high-pressure cylinder, and the size of the chambers had no influence on the detection of the transition pressures. Phase diagrams of binary systems of gases were also made by using this double sonic-chamber technique, as mentioned in the following section. As to the ultrasound velocity, the measurements were very accurate at a gas-gas separation, since the separation could proceed rapidly through the holes of the sonic chambers. However, in the case of solidification, measurements were largely disturbed by the precipitation of solids on the piezo-electric crystals.

#### 4.3 Phase diagram

There are different kinds of transitions in the binary systems of gases. Freezing is one of the first-order transitions in which both the volume and the velocity change discontinuously. Another kind is a phase separation in which a homogeneous gas mixture separates into two phases of either gases or a gas and a solid of different densities and concentrations, and no discontinuous change of the volume occurs. In the case of the univariant reactions in which three phases become in equilibrium,

discontinuities in both the volume and the velocity take place. In this experiment, in order to distinguish these kinds of transitions from each other, the volume changes, the ultrasound velocity changes, and sudden changes of the wave form and amplitude of the pulses displayed on an oscilloscope were examined during the run. Then, after the experiment, the data of the pressure, volume and velocities were compared together with the wave form and amplitude changes to identify the nature of the transitions. There has been no problem in determining whether the transition was gas-gas or gas-solid.

To make the phase diagram of a binary system, the pressures of the transition were plotted against the concentration. In Fig. 17, the actual data versus the concentration for krypton and helium gas mixtures up to 1.6 GPa is shown. The procedures to obtain the data will be described in detail in §5.6.

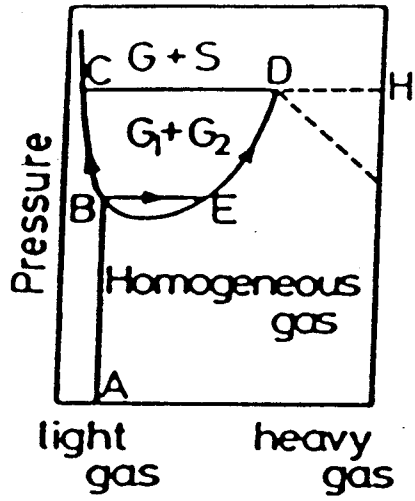


Fig. 1 (a)

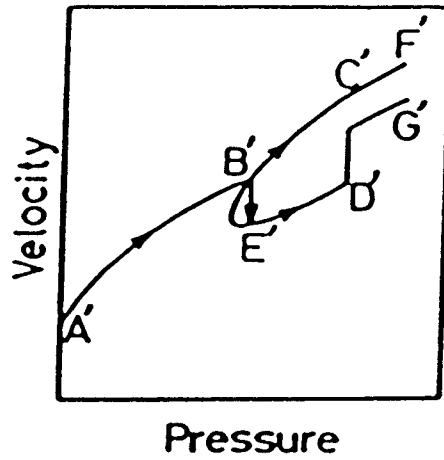


Fig. 1 (b)

Fig. 14 Phase separation of a gas mixture. (a) Pressure-concentration phase diagram of a binary system. (b) Expected sound velocity versus pressure relation.

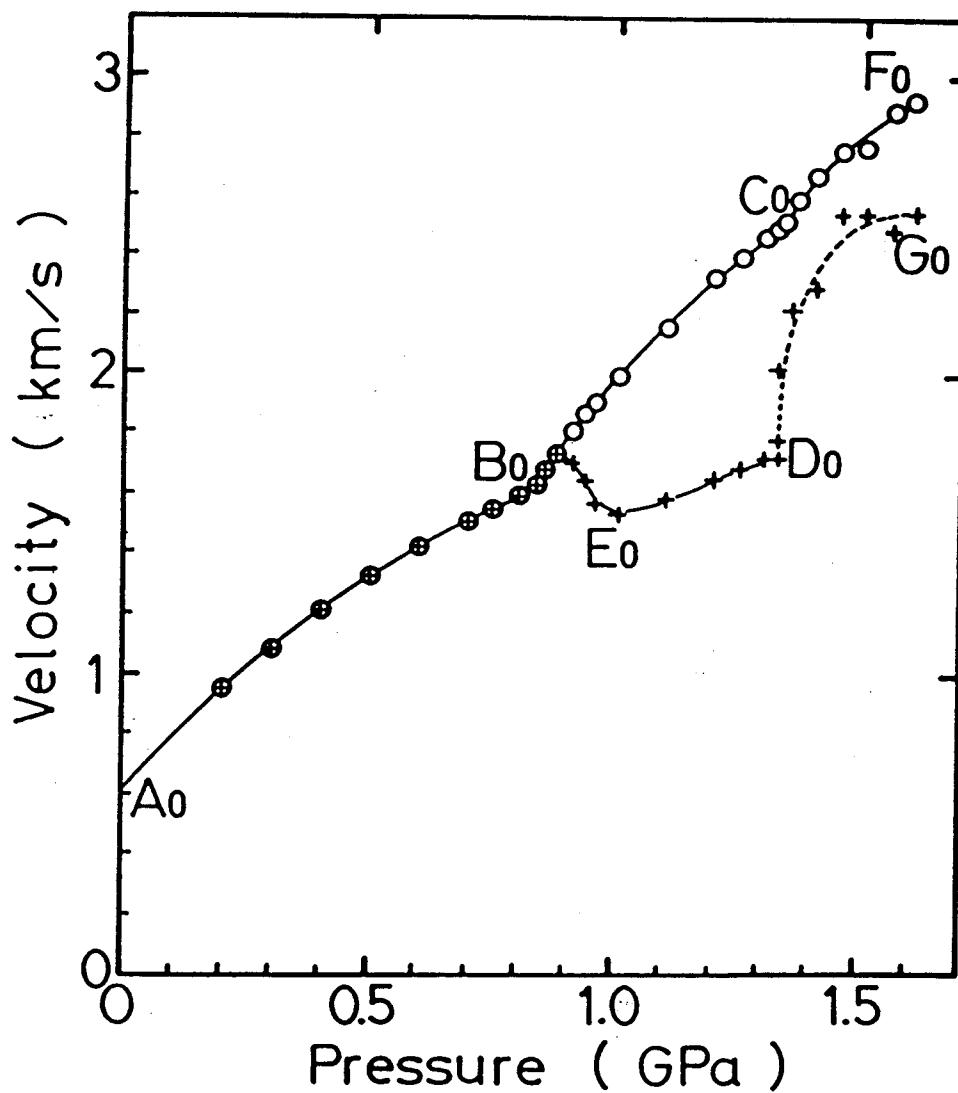


Fig. 15 Sound velocity changes at phase separation and solidification of krypton-herium mixed gas, containing 15 percent krypton, at 20 °C.

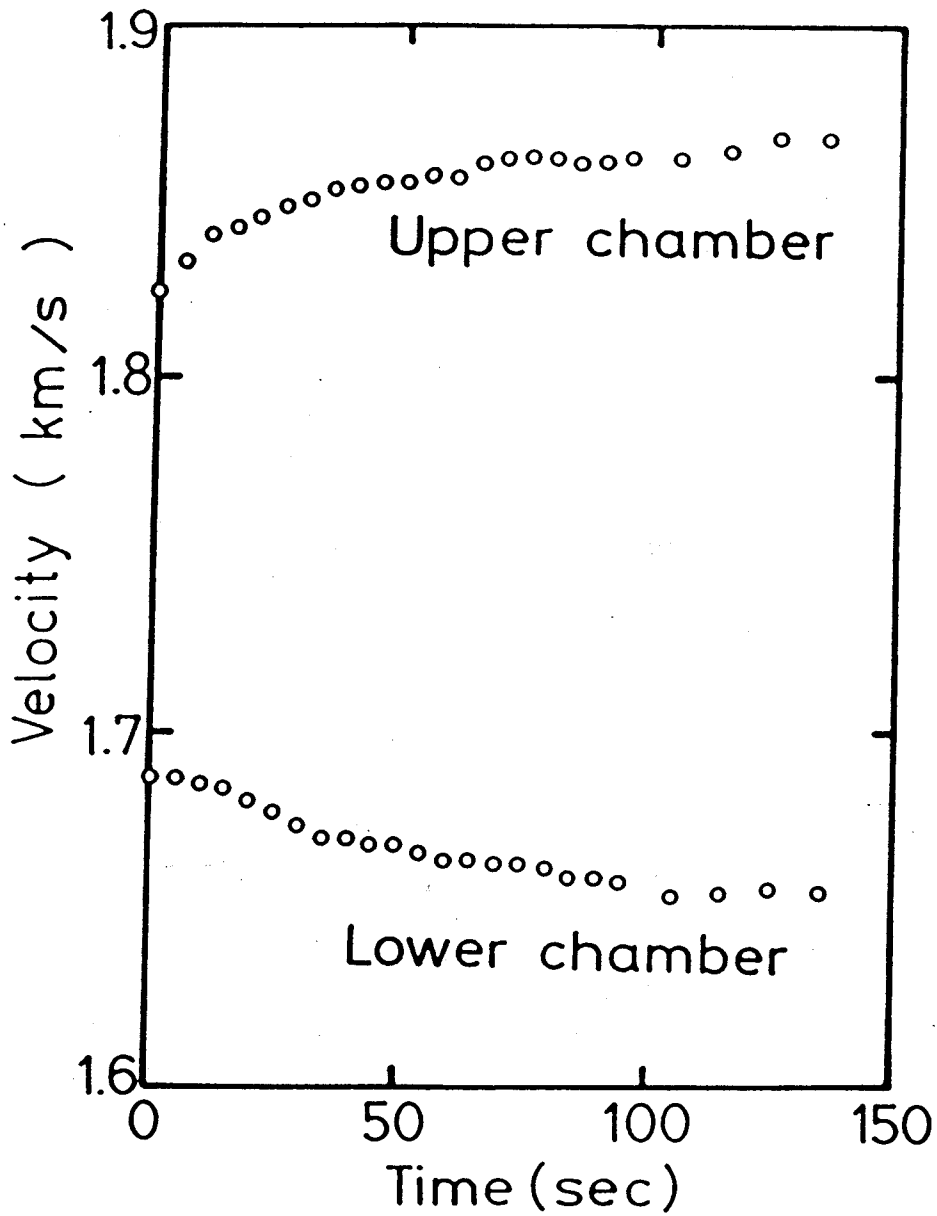


Fig. 16 Example of time variation of sound velocity in the krypton-85 percent helium mixture at 912 MPa, when increasing pressure.



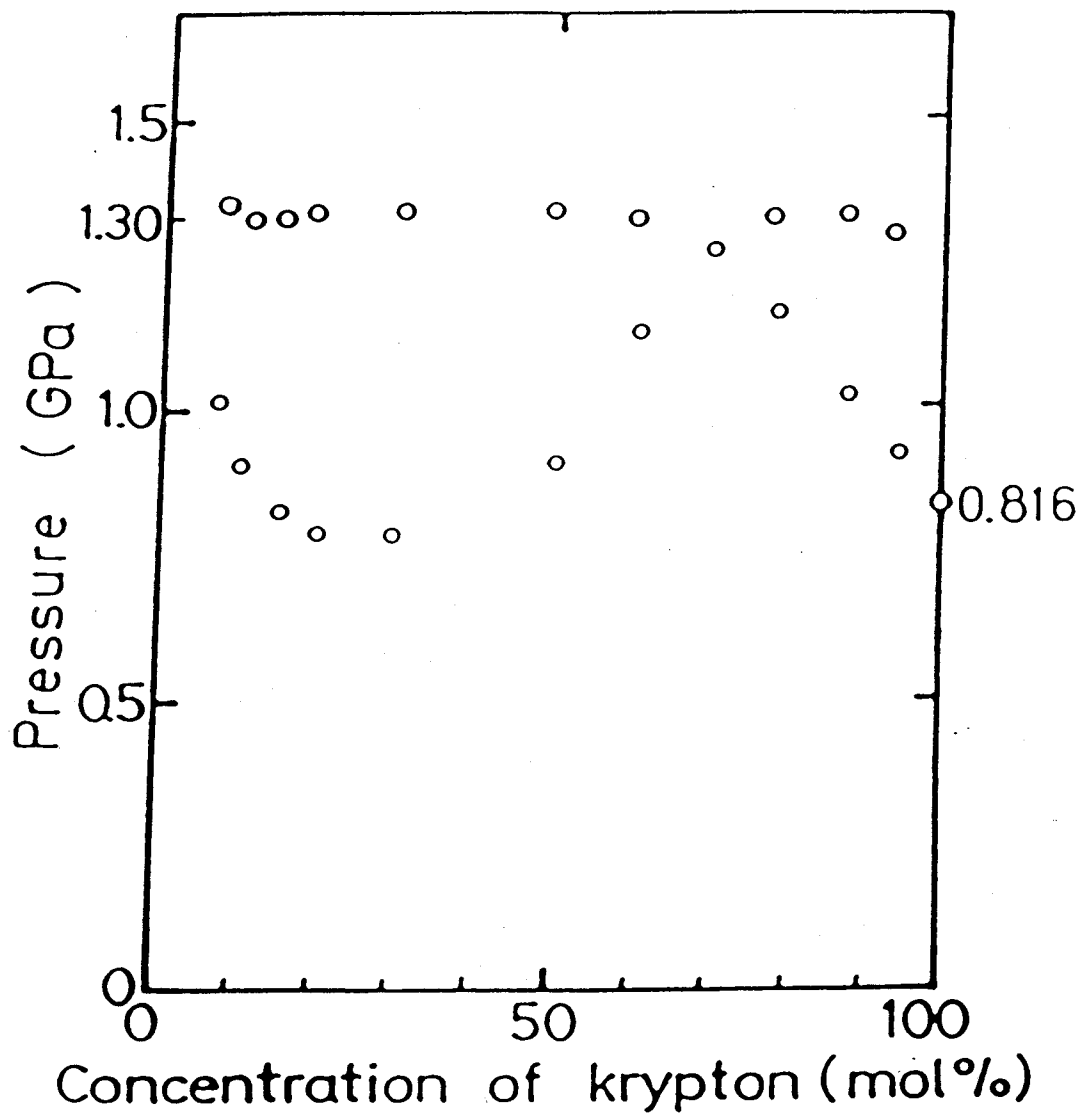


Fig. 17 A plot of the transition pressures versus concentration from the sound velocity measurement of krypton-helium mixtures at 20 °C.

## §5. Results

### 5.1 Test of gas apparatus

A number of pre-experiment runs were made using argon, nitrogen, neon, and helium gas at room temperature. In the first few runs, leakage occurred in the packings at the bottom closure at above 2.9 GPa, presumably because the steel ring was permanently deformed and no unsupported area remained below it at this pressure. This was improved by using 300 maraging steel together with the change of the design as mentioned before. Several runs were also made at temperatures up to 800 °C and pressures up to 3 GPa. No trouble was encountered in these temperature and pressure ranges.

### 5.2 Discussion on strength of the cylinder

A simple calculation using continuum elastic theory <sup>71)</sup> was applied in order to check the strength of the high-pressure vessel as follows. Consider that a long elastic cylinder with the bore radius  $r_i$  and the outside diameter  $r_o$  is subjected to an internal gas pressure  $P_i$  and an external pressure  $P_o$ . Using the wall ratio  $\omega = r_o/r_i$ , the maximum stress difference  $S_D$ , which appears at the radial distance  $r_i$ , is given by

$$S_D = 2(P_i - P_o) \frac{\omega^2}{\omega^2 - 1} \quad (3)$$

The maximum stress difference should not exceed the yield point  $S_y$  of the material of the cylinder for indefinite uses. The condition is shown as

$$S_D \leq S_y \quad (4)$$

If we take into account the residual stress  $P_r$  produced in the overstrained cylinder, which will compress the cylinder inward as  $P_o$ , eq. (3) becomes

$$S_D = 2(P_i - P_o - P_r) \frac{\omega^2}{\omega^2 - 1} \quad (5)$$

Though estimation of  $P_r$  is difficult, we may assume that, after many runs of the high pressure experiment conducted above the yield point,  $P_r$  will become nearly equal to  $S_y / 2$ .<sup>72)</sup> For the cylinder used in the present experiment, the following values can be used;  $S_y \approx 2.4$  GPa,  $P_o = 1.8$  GPa,  $P_r \approx 1.2$  GPa and  $\omega = 6$ . Then, eq. (5), gives  $P_i \leq 4.2$  GPa, which shows that the cylinder can be used up to 4 GPa.

After exposures to pressures above 3.0 GPa, the cylinder bore was enlarged by 0.1 mm in diameter. This could give rise to a too large expansion of clearance and accordingly an unimproved leakage from the packings. However, it is not the case, because at the portions just above and below the pressurized part of the cylinder, where we can assume  $P_i = 0$ , the above enlargement will not take place, as mentioned below. At the above portions, the radial displacement  $u$  at  $r = r_i$  is approximately given by

$$u = \frac{-2}{Y} P_o \frac{\omega^2}{\omega^2 - 1} r_i \quad (6)$$

where  $Y$  is the Young's modulus. For the cylinder used in the experiment,  $P_o$  given by the compression by the support ring, is nearly equal to 1.8 GPa and  $r_i = 10$  mm, so that we get  $u = -0.18$  mm

from eq. (6). This value exceeds the above-mentioned enlargement of the bore by the applied internal pressure, therefore, no leakage will occur at all.

### 5.3 Freezing point of nitrogen and krypton gas at room temperature

The purities of both nitrogen and krypton gases used in the experiment were more than 99.99 percent. To measure the ultrasound velocity, only the lower sonic chamber with a 20 mm-spacer was used in the case of nitrogen, and two sonic chambers for pure krypton, as described in the preceding paragraphs. The velocity of ultrasound waves and the volume of nitrogen gas at  $22 \pm 0.3$  °C were measured up to 2.6 GPa.

In Table I, the velocity and piston displacement versus pressure for nitrogen gas are given. The data were obtained from the mean values of two runs, between which the differences were within 0.2 percent. The velocity increased smoothly with pressure up to 2.29 GPa but at 2.38 GPa they changed discontinuously with an increment of about 10 percent, as shown in Fig. 18. The freezing pressure of nitrogen  $P_f$  at 22 °C was therefore given as  $2.29 \text{ GPa} \leq P_f \leq 2.38 \text{ GPa}$ . The velocities on decreasing pressures could not be obtained except for one value, 3453 m/s at 2.463 GPa. In the experiment of pure gases, either the pulse circuits or the piezo-electric crystals were often broken at solidification, so that the freezing pressure data could not be obtained for decreasing pressure from velocity measurement.

The piston displacement relative to the high-pressure cylinder was measured with two electric micrometers. The

measurements were carried out for both increasing and decreasing pressure. When increasing the pressure,  $P_f$  was determined as  $2.29 \text{ GPa} \leq P_f \leq 2.35 \text{ GPa}$  by a discontinuous movement of the piston. When lowering the pressure, more precise measurement was done and the discontinuous movement was found to be as much as 1.2 mm at 2.329 GPa, an example being shown in Fig. 19(a). The data on  $P_f$  from two runs were in good agreement within 0.02 GPa.

Other data on the freezing pressure were obtained from a direct reading of the pressure gauge. When the pressure was increased no clear change was found, but when decompressing the gas stepwise (Fig. 19(b)), the pressure showed a slight increase just below the freezing pressure, becoming constant at  $2.329 \pm 0.02 \text{ GPa}$  within a few minutes. This pressure change arose from the gasification or sublimation of solid to increase the pressure, and accordingly the reached constant pressure was no other than the freezing pressure. When the gasification was over, pressure change disappeared.

From the above three kinds of data, it is concluded that the freezing pressure of nitrogen is given as  $2.29 \text{ GPa} \leq P_f \leq 2.35 \text{ GPa}$ ; the more exact recommended value is  $2.329 \text{ GPa} \pm 0.02 \text{ GPa}$ .

The volume change of nitrogen gas under high pressure was calculated from the piston displacement. The present experiment started from a pressure of about 300 MPa, and the absolute values of the volume of the gas below 400 MPa were determined so as to fit the accurate data in this pressure range by Morris and Wylie.<sup>73)</sup> At the freezing point, the volume of nitrogen decreased by 2.0 percent. Therefore, the molar volumes of nitrogen gas and solid at 2.329 GPa at 22 °C are  $20.9 \text{ cm}^3/\text{mol}$ , and  $20.5 \text{ cm}^3/\text{mol}$ ,

respectively. In Table II, the pressure dependence of the volume of nitrogen at 22 °C is shown.

Regarding krypton gas, the same procedure was taken by employing the standard values of volume given by Trappeniers, Wassenaar and Wolkers.<sup>74)</sup> The pressure dependence of the ultrasound velocity and the volume of krypton gas at  $20 \pm 0.3$  °C are shown in Table III and Fig. 20. The freezing pressure of krypton gas at 20 °C was determined as  $816 \pm 10$  MPa from the data of both the velocity and piston displacement. From a direct reading of the pressure gauge, the freezing pressure could not be obtained in the case of krypton.

The results were compared with previously published data by other investigators, as follows. The ultrasound velocity of pure nitrogen gas was measured by Voronov, Pitaevskaya and Bilevich<sup>75)</sup> and Mills, Liebenberg and Bronson<sup>43)</sup> up to 0.4 and 2.2 GPa, respectively. The present data differ by a maximum of 1.0 percent with an average of 0.2 percent from the data by Voronov et al.<sup>75)</sup> and by a maximum of 0.7 percent with an average of 0.4 percent from the data by Mills et al..<sup>43)</sup>

The freezing pressures of nitrogen gas at room temperature and 273.3 K were measured by Birch and Robertson<sup>36)</sup> and Mills et al.,<sup>44)</sup> respectively. The present data differ by 15 percent from the data by Birch and by 1.3 percent from the data by Mills et al.<sup>44)</sup> extrapolated to 22 °C. The volume of nitrogen gas at room temperature were measured by Mills et al.,<sup>43)</sup> and the present data differ from that data by 0.6 percent.

The ultrasound velocity and the volume of pure krypton under high pressure were measured by Vidal, Tufeu, Garrabos and

Neindre<sup>76)</sup> and the present data differ from their data in the case of the velocity by an average of 0.2 percent and in the case of the volume by 1.4 percent. The freezing point of krypton gas obtained by Lahr and Eversole,<sup>68)</sup> and that by Crawford and Danniels<sup>69)</sup> extrapolated to 20 °C differ from the present datum mentioned before by about 1.4 percent and about 1.2 percent, respectively.

It is worthy of note that no appreciable deformation of the cylinder vessel nor leakage from it took place even in the highest pressure range and measurements of volume, ultrasound velocity and pressure were repeated with the slightest errors, as mentioned before, and, accordingly, the author believes that all the experimental data obtained in the present study are presumably the most reliable ones among others by other investigators.

#### 5.4 Velocity of ultrasound waves in pure neon gas up to 3.5 GPa

In the present experiment, neon gas of more than 99.99 percent purity was used. Chemical analyses were performed before and after the experiment. To measure the ultrasound velocity, only the lower sonic chamber with a 20 mm-spacer was used, as well as in the case of nitrogen. For the calibration in the volume measurement of neon the data obtained by Vidal et al.<sup>76)</sup> at 1 GPa were utilized. In Table IV and also in Fig. 21, the ultrasound velocity in neon at  $22 \pm 0.3$  °C is shown. The velocity increased smoothly with pressure up to 3.5 GPa, the rate of increase slowing down; however solidification could not be obtained.<sup>77)</sup> Values of the molar volume of neon gas are shown in

Table V and Fig. 22 up to 3.5 GPa.

Vidal et al.<sup>76)</sup> have studied the rare gases under high pressure, and their ultrasound velocity data on neon gas are in good agreement with the present data within 0.7 percent except at very low pressures.

Empirical equations of the sound velocity in monoatomic gas as a function of the pressure or volume have been postulated in different forms. In the free-volume model,<sup>80)</sup> the velocity will be inversely proportional to the cubic root of the volume approximately. Liebenberg et al.<sup>81)</sup> suggested from their experimental results that the velocity is inversely proportional to the volume itself. Takagi<sup>82)</sup> presented an empirical equation for the variation of the velocity in liquid as a cubic form of pressure. Nishitake and Hanayama<sup>83)</sup> have measured the velocities of ultrasound waves in pure helium, argon up to 1.5 and 1.3 GPa, respectively, and also in pure xenon gas up to 0.4 GPa.<sup>69)</sup> In Fig. 23, the data of the present experiment on krypton and neon gas are shown together with the data cited above. In the case of an ideal gas under relatively low pressure, it is generally known that the sound velocity is given by

$$U = \sqrt{\gamma PV/M} \quad (7)$$

Here  $\gamma$ ,  $P$ ,  $V$  and  $M$  are the heat-capacity ratio, the pressure, the molar volume, and the molecular weight, respectively. However, the obtained data of sound velocities did not agree with the above equation but with an empirical formula:



$$U = \sqrt{\gamma PV/M + (V_0/V)^2 b} \quad , \quad (8)$$

where  $\gamma$  ,  $V_0$  and  $b$  are 1.67, the molar volume at atmospheric pressure, and a constant around unity, depending upon the measured gas, respectively. Under very low pressure the present experimental data seemed to follow the eq.(7), but as soon as the pressure was raised over about 100 MPa disagreement between the data and the equation became so large that the former was not reliable at all. Therefore, we proposed the eq.(8), which gives good agreements with the experiments, as shown in Fig. 23, where the constant  $b$ 's are determined from the best fits and given in Table VI.

### 5.5 Velocity of ultrasound wave in mixture of krypton-helium gas

More than a dozen of runs for different concentrations were made using 99.99 percent pure krypton and helium. Chemical analyses were done before and after each experiment, but after the separation and mixing again of gases, no plausible result of analysis was obtained because it took a long time, the order of a few days, for mixing to achieve a mixture homogeneous enough for chemical analysis. The sound velocities in gas mixtures containing 8, 10, 15, 20, 30, 50, 60, 70, 78, 87 and 93 mole percentage of krypton were measured up to 1.6 GPa at 20 °C. In Table VII, velocities of the krypton-helium gas mixtures at the lower and upper sonic chambers are shown at  $20 \pm 0.3$  °C up to 1.6 GPa. All the data were obtained during the process of compressing. The data obtained during decompression was not always reproducible, since the re-mixing of gases was extremely slow (as mentioned above).

Differing from the measurements for pure gases, no trouble occurred during solidification on both the electric circuits and piezo-crystals probably because the mixture of solid and gas was soft enough to prevent breaks of them.

Using a small apparatus<sup>38)</sup> and also a lower sonic chamber, measurements of the velocities were made below 200 MPa as shown in Table VIII. The velocities at pressures between 10 MPa and 800 MPa are shown in Fig. 24, where the mixtures of gases were homogeneous. At a pressure of about 30 MPa, the data showed that the velocities in the mixed gas had a minimum value with respect to mole percentage of about 60 percent krypton in all the cases.

#### 5.6 Phase separation and phase diagram of mixture of krypton-helium gas

Phase separation and solidification occurred in almost all runs, and the transition pressures were determined either by only the velocity or both the velocity and the piston movement.

A phase-transition without a volume change could be detected by measuring only the velocity. In Fig. 25, the velocity versus pressure diagram for mixtures with less than 70 percent krypton are shown; the pressures of the transition from the homogeneous gas phase to two different gas-phases, which accompanied no volume change, are clearly identified.

For the contents of more than 70 percent krypton, the solidification occurred two times in one run. The one accompanied no volume change, and for the other the discontinuous volume-change was measured by the piston movement. In Fig. 26, the velocity versus pressure curves are shown, where the short arrows

indicate the transition pressures from the homogeneous gas phase to gas-solid mixture phase accompanying no volume change. In Table IX, the transition pressures without volume change is shown.

With respect to the first-order transitions in which a volume change could be observed, the transition pressures were determined by both the velocity and the piston displacement. The univariant three-phase equilibrium pressure  $P_3$  obtained from the velocity measurement are shown in Table X. For the concentrations less than 70 percent krypton, the already separated two gas-phases changed to the three-phases at  $P_3$ , which is shown by an arrow in Fig. 25. For the concentrations more than 70 percent krypton, the pre-existed gas-solid phases changed to the gas-gas-solid phases at  $P_3$  (shown by a long arrow in Fig. 26). The mean value of the univariant pressures  $P_3$  obtained by the velocity measurements was 1302 MPa with the standard deviation of 11 MPa.

Abrupt changes of the volume occurred during solidification at the three-phase equilibrium line. The three-phase equilibrium pressures obtained from the piston displacement, were 1299, 1300, 1300, 1278 and 1296 MPa in the cases of 60, 70, 78, 87 and 93 percent krypton content, respectively. The mean value of the above data was 1295 MPa with the standard deviation of 8 MPa. The difference between the pressures obtained from the velocity and piston displacement was only 7 MPa. From the above measurements, the univariant pressure was determined as  $1300 \pm 11$  MPa.

In Fig. 27, a phase diagram of krypton-helium system is shown, using the data shown in Fig. 17 and Tables IX and X. The lowest point of the gas-gas separation is at 0.78 GPa at 27

percent krypton, and the widest separation takes place at 1.30 GPa between about 5 percent and 68 percent krypton gas. The solid phase is almost of pure krypton and helium content of the solid was not confirmed.

Since the first success by Arons and Diepen<sup>57)</sup> in the gas-gas separation under high pressure, many papers<sup>58-60, 84, 85)</sup> have been published. But, there scarcely exists the amount of data available at high pressures above 1 GPa. Helium-krypton gas mixture were measured up to 12 MPa in a temperature range from 100 to 150 K by Kidnay et al..<sup>84)</sup> And helium-krypton gas mixture were measured up to 15 MPa in a temperature range from -50 to 50 °C by Dillard et al..<sup>85)</sup> In the present study, the volume and the sound velocity change of the krypton and helium gas mixture under high pressures up to 1.6 GPa were precisely measured with high accuracy and a reliable concentration-pressure diagram was completed.

Table 1. Sound velocities  $U$  when raising pressures and piston displacements  $d$  at decompressing in nitrogen gas as functions of pressure  $P$  at 22 °C.

$P$ (MPa)	$U$ (m/s)	$P$ (MPa)	$d$ (mm)
291	1387	394	17.685
389	1559	584	26.019
785	2073	771	31.119
1176	2388	969	35.804
1483	2613	1186	39.773
1779	2793	1372	42.739
2089	2937	1581	45.756
2291	3018	1770	48.194
2382	3283	1974	50.579
2442	3398	2220	53.134
2489	3457	2305	54.057
2533	3493	2329	54.914
2647	3604	2382	55.789
		2464	56.572
		2580	57.318
		2678	58.160

Table II. Molar volumes  $V$  of nitrogen at 22 °C as a function of pressure  $P$ , from the data at lowering pressure.

$P$ (MPa)	$V$ (cm <sup>3</sup> /mol)
394	31.79
584	28.82
771	27.02
969	25.54
1186	24.41
1372	23.06
1581	22.80
1770	22.20
1974	21.62
2220	21.06
2305	20.82
2329	20.56
2382	20.32
2464	20.13
2580	20.06
2678	19.94

Table III. Sound velocities  $U$  and molar volumes  $V$  of krypton as functions of pressure  $P$  at 20 °C.

$P$ (MPa)	$U$ (m/s)	$V$ (cm <sup>3</sup> /mol)
198	835	36.48
245	900	34.87
293	966	33.58
343	1018	32.49
390	1072	31.62
441	1122	30.81
491	1158	30.12
538	1201	29.59
588	1231	29.09
634	1268	28.57
681	1300	28.18
733	1336	27.73
781	1362	27.36
813	1381	26.92
821	1415	26.25
832	1735	25.62

Table IV. Sound velocities  $U$  of neon gas as a function of pressure  $P$  at 22 °C.

$P$ (MPa)	$U$ (m/s)
196	917
291	1034
339	1121
683	1486
822	1580
980	1681
1481	1939
1967	2159
2482	2345
2757	2434
2984	2511
3146	2536
3300	2607
3495	2728



Table V. Molar volumes  $V$  of neon gas as a function of pressure  $P$  at 22 °C.

$P$ (MPa)	$V$ (cm <sup>3</sup> /mol)
683	15.00
822	14.06
980	13.22
1481	11.54
1511	11.47
1785	10.80
1966	10.48
2541	9.74
2757	9.39
2948	9.25
3146	9.13
3300	8.95
3496	8.80

Table VI. Constant  $b$  in the eq. (8).

	$b \text{ ( m}^2/\text{s}^2 \text{ )}$
He	0.83
Ne	0.59
Ar	2.24
Kr	1.83
Xe	2.44

Table VII. Velocities of ultrasound waves  $U_1$  and  $U_2$  obtained in the upper chamber and lower one of krypton-helium mixtures as the functions of pressure  $P$  at 20 °C for raising pressure, respectively.

a) 8-15 percent krypton

Concentration of krypton ( mole percentage )								
8			10			15		
P	$U_1$	$U_2$	P	$U_1$	$U_2$	P	$U_1$	$U_2$
(MPa)	(m/s)	(m/s)	(MPa)	(m/s)	(m/s)	(MPa)	(m/s)	(m/s)
199	1125	1121	195	1032	1029	194	947	948
302	1284	1288	292	1194	1192	290	1082	1082
390	1429	1423	388	1322	1316	391	1216	1215
482	1545	1537	488	1451	1442	487	1329	1329
602	1689	1681	586	1551	1543	584	1433	1430
681	1750	1750	683	1649	1639	684	1519	1515
786	1871	1866	783	1738	1730	731	1565	1560
900	1955	1945	829	1778	1772	758	1576	1572
988	2026	2011	879	1835	1823	785	1604	1598
1109	2153	2120	900	1856	1847	810	1628	1620
1315	2460	2412	922	1900	1896	832	1677	1669
1341	2553	2518	940	1948	1932	857	1743	1736
			957	1972	1967	890	1812	1709
			978	1986	1990	912	1864	1643
			1029	2078	2073	936	1904	1572
			1076	2148	2144	981	2001	1542
			1127	2223	2222	1075	2158	1586
			1177	2299	2288	1178	2330	1658
			1227	2361	2362	1227	2399	1694
			1259	2403	2399	1278	2468	1734
			1289	2438	2433	1299	2488	1734
			1313	2510	2514	1304	2521	1783
			1329	2542	2536	1312	2514	2029
			1392	2613	2619	1338	2605	2229
						1382	2675	2295
						1431	2765	2545
						1481	2771	2536
						1533	2895	2483
						1590	2923	2563

Table VII. (continued).

## b) 20-50 percent krypton

Concentration of krypton ( mole percentage )								
20			30			50		
P	U <sub>1</sub>	U <sub>2</sub>	P	U <sub>1</sub>	U <sub>2</sub>	P	U <sub>1</sub>	U <sub>2</sub>
(MPa)	(m/s)	(m/s)	(MPa)	(m/s)	(m/s)	(MPa)	(m/s)	(m/s)
200	886	890	194	812	811	195	779	782
290	1013	1008	296	958	955	309	932	925
390	1131	1132	388	1071	1065	411	1048	1046
492	1248	1243	486	1176	1168	509	1161	1157
584	1336	1333	585	1257	1248	609	1214	1206
687	1434	1432	682	1329	1329	743	1319	1321
736	1464	1459	781	1404	1410	847	1373	1370
783	1497	1496	876	1722	1435	950	1454	1442
832	1627	1424	982	1957	1498	1041	1534	1499
878	1761	1459	1074	2133	1570	1135	1640	1587
932	1874	1504	1185	2295	1625	1235	1802	1659
981	1964	1537	1279	2430	1708	1322	1978	1682
1030	2064	1572	1364	2625	1778	1438	2310	1820
1076	2114	1581	1467	2800	2072	1549	2545	2104
1175	2257	1643	1595	2841	1931			
1278	2389	1710						
1315	2446	1738						
1366	2531	2014						
1498	2855	2161						

Table VII. (continued).

c) 60-78 percent krypton

Concentration of krypton (mole percentage )								
60			70			78		
P	U <sub>1</sub>	U <sub>2</sub>	P	U <sub>1</sub>	U <sub>2</sub>	P	U <sub>1</sub>	U <sub>2</sub>
(MPa)	(m/s)	(m/s)	(MPa)	(m/s)	(m/s)	(MPa)	(m/s)	(m/s)
191	754	750	200	783	782	194	788	784
292	890	886	326	956	956	290	935	927
390	1002	998	397	1047	1041	388	1028	1028
490	1101	1094	491	1140	1138	491	1120	1120
583	1186	1180	586	1209	1207	588	1197	1195
676	1249	1241	690	1290	1289	689	1276	1268
782	1327	1321	787	1348	1343	788	1337	1331
880	1386	1378	885	1406	1406	881	1387	1379
941	1415	1410	989	1461	1456	982	1447	1438
984	1440	1436	1033	1484	1485	1076	1495	1488
1029	1466	1461	1085	1498	1492	1099	1506	1502
1076	1490	1483	1129	1520	1516	1125	1514	1511
1128	1521	1521	1180	1545	1538	1142	1528	1526
1174	1534	1533	1266	1594	1593	1163	1530	1533
1218	1565	1549	1365	1734	1746	1177	1576	1568
1248	1582	1571	1413	2006	—	1190	1595	1579
1277	1587	1585	1475	2004	—	1240	1644	1659
1295	1628	1610				1270	1691	1686
1317	2192	2193				1276	1694	1734
1343	2207	2201				1288	1708	1742
1367	2184	2165				1344	1993	1991
1431	2199	2158				1407	2055	2141
1482	2203	2166				1447	2100	2117
						1487	2101	2098

Table VII. (continued).

## d) 87-93 percent krypton

Concentration of krypton (mole percentage)					
87			93		
P	U <sub>1</sub>	U <sub>2</sub>	P	U <sub>1</sub>	U <sub>2</sub>
(MPa)	(m/s)	(m/s)	(MPa)	(m/s)	(m/s)
193	801	800	192	823	821
294	933	934	292	948	948
391	1044	1042	387	1051	1053
492	1139	1137	487	1141	1143
586	1208	1204	586	1217	1218
687	1283	1278	680	1284	1279
783	1340	1334	773	1345	1343
876	1395	1394	814	1370	1365
930	1418	1418	838	1380	1378
957	1436	1432	857	1395	1391
981	1451	1447	879	1409	1406
999	1457	1453	906	1419	1419
1023	1470	1467	923	1430	1431
1029	1501	1495	942	1485	1480
1050	1526	1536	964	1525	1522
1074	1566	1562	991	1531	1554
1121	1612	1624	1017	1577	1591
1167	1633	1673	1035	1584	1604
1216	1677	1702	1075	1620	1623
1252	1720	1728	1125	1640	1664
1277	1732	1751	1174	1681	1702
1291	1740	1733	1223	1694	1757
1309	1788	1880	1278	1745	1769
1344	1922	1944	1294	1788	1830
			1328	1852	1892
			1379	1859	1951
			1439	1926	1943

Table VIII. Velocities of ultrasound waves U in krypton-helium gas mixtures of homogeneous phase, as a function of the concentration of krypton x at pressure P between 10 and 800 MPa at 20 °C. The values for x=0 (pure helium) are measured at 25 °C.<sup>83)</sup>

P (MPa)	x (mole percentage)												
	0	8	10	15	20	30	50	60	70	78	87	93	100
U (m/s)													
10	1038	665	609	532	470	401	326	297	272	260	246	240	220
20	1082	687	639	561	501	427	352	323	298	291	283	284	271
30	1125	718	668	590	532	455	380	354	330	328	330	337	338
40	1165	747	696	617	558	484	408	386	365	368	378	389	402
50	1204	776	723	643	582	513	437	420	401	408	424	439	460
60	1242	804	750	668	606	541	465	452	436	448	468	483	509
70	1278	832	776	693	629	569	493	484	470	486	508	524	551
80	1312	860	802	717	655	595	519	514	502	522	545	559	586
90	1346	885	826	740	679	620	545	543	531	556	577	591	615
100	1378	910	850	763	705	643	569	570	559	587	607	620	641
110	1410	934	873	785	724	665	592	595	584	616	634	646	665
120	1440	958	896	806	742	686	614	618	608	643	659	669	690
130	1470	980	917	827	766	706	635	640	630	668	682	692	713
140	1499	1002	938	847	786	725	655	660	650	690	703	713	739
150	1527	1022	958	866	807	743	675	679	670	710	723	733	762
160	1555	1044	978	886	819	760	693	697	690	728	741	753	781
170	1581	1063	996	904	835	778	712	713	710	744	759	771	802
180	1607	1082	1014	922	857	796	730	729	730	758	776	789	815
190	1633	1100	1031	940	873	814	748	745	752	771	793	804	831
200	1657	1116	1047	956	891	834	766	761	775	783	807	815	846

Table IX. Experimental results on the pressures of gas-gas phase separation  $P_s$  and of gas-solid separation  $P_f$  on krypton-helium mixture at 20 °C as a function of the concentration of krypton  $x$ , from the sound velocity measurement.

$x$ (mole percentage)	$G \rightarrow G_1 + G_2$ $P_s$ (MPa)	$G \rightarrow G + S$ $P_f$ (MPa)
8	988	
10	900	
15	811	
20	783	
30	781	
50	890	
60	1128	
70		1266
78		1163
87		1023
93		923



Table X. Experimental results on the univariant three-phase equilibrium pressure  $P_3$  of krypton-helium mixtures at 20 °C as a function of the concentration of krypton  $x$ , from the sound velocity measurement. G: gas, S: solid,  $G_1$ ,  $G_2$ : two gas phases. The datum in the parentheses was obtained from the piston displacement.

$x$ (mole percentage)	$G_1 + G_2 \longrightarrow G_1 + G_2 + S$ $P_3$ (MPa)	$G + S \longrightarrow G_1 + G_2 + S$ $P_3$ (MPa)
8	1315	
10	1294	
15	1304	
20	1306	
30	1306	
50	1322	
60	1299	
70		(1300)
78		1300
87		1298
93		1278

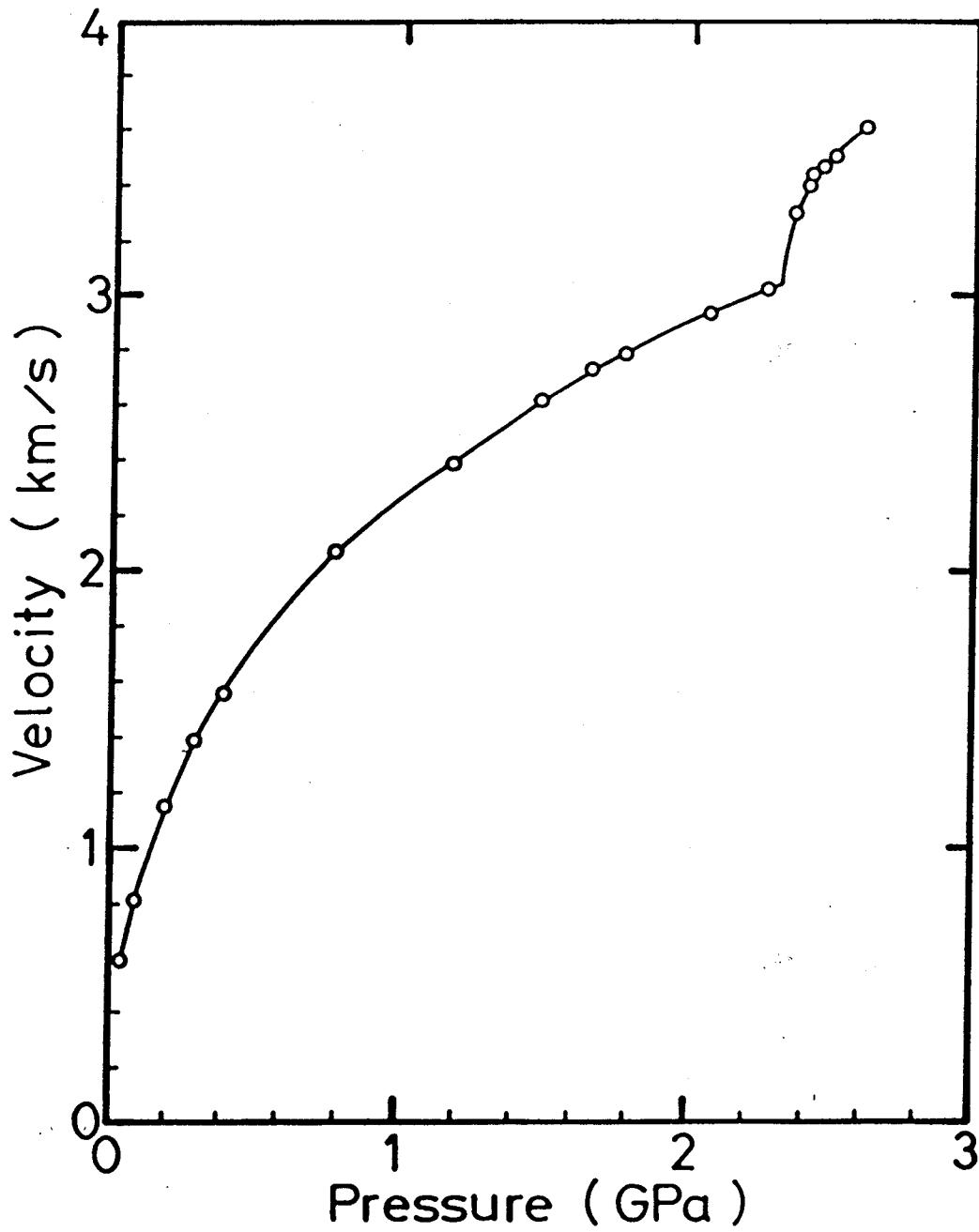


Fig. 18 Velocity of ultrasound waves in nitrogen versus pressure at 22 °C.

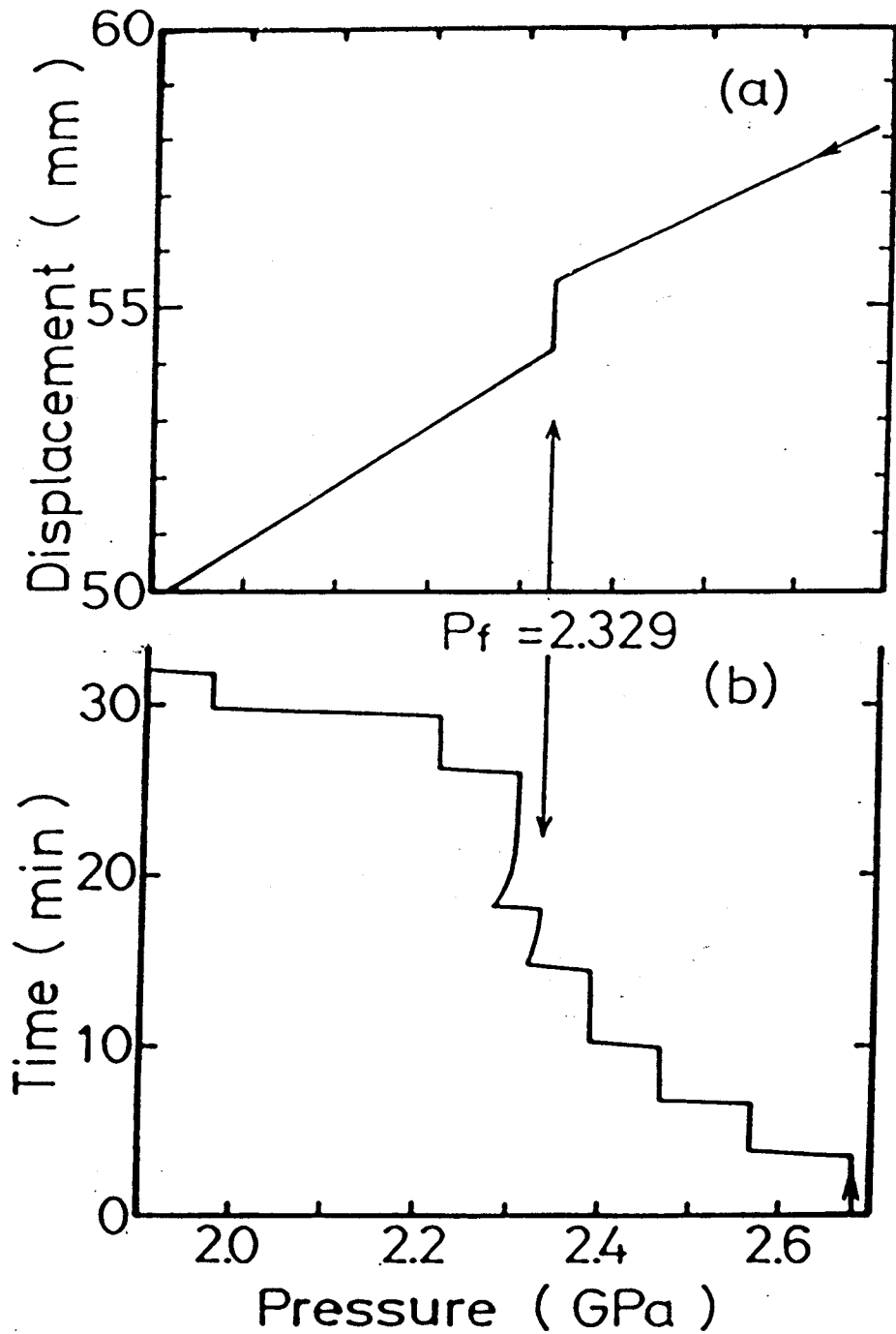


Fig. 19 (a) Piston displacement versus pressure for nitrogen showing a discontinuity at the gas-solid transition. (b) Pressure change of nitrogen gas during stepwise decreasing of pressure measured by a manganin pressure gauge.

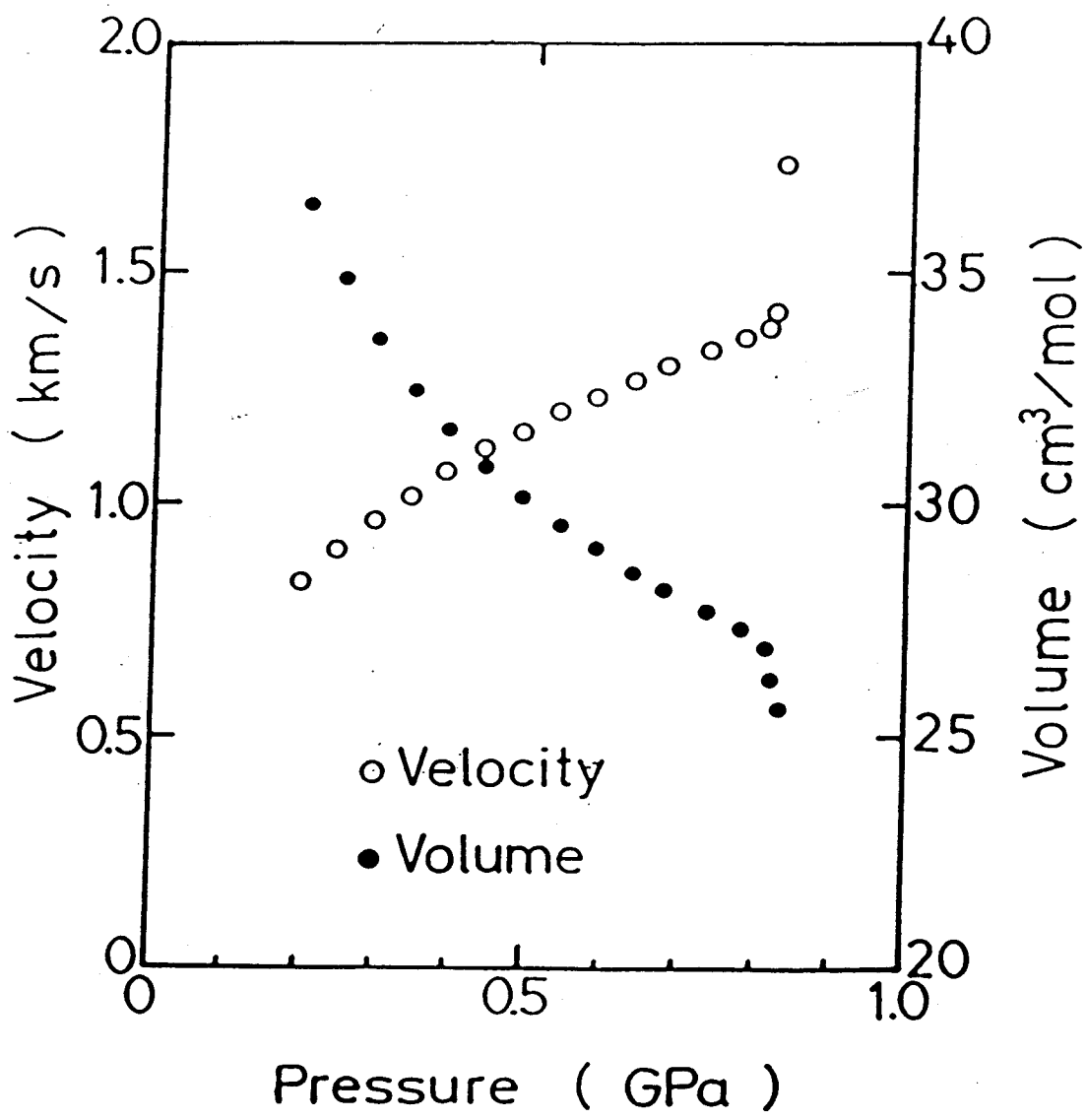


Fig. 20 Sound velocity and volume change of krypton as the functions of pressure at 20 °C.

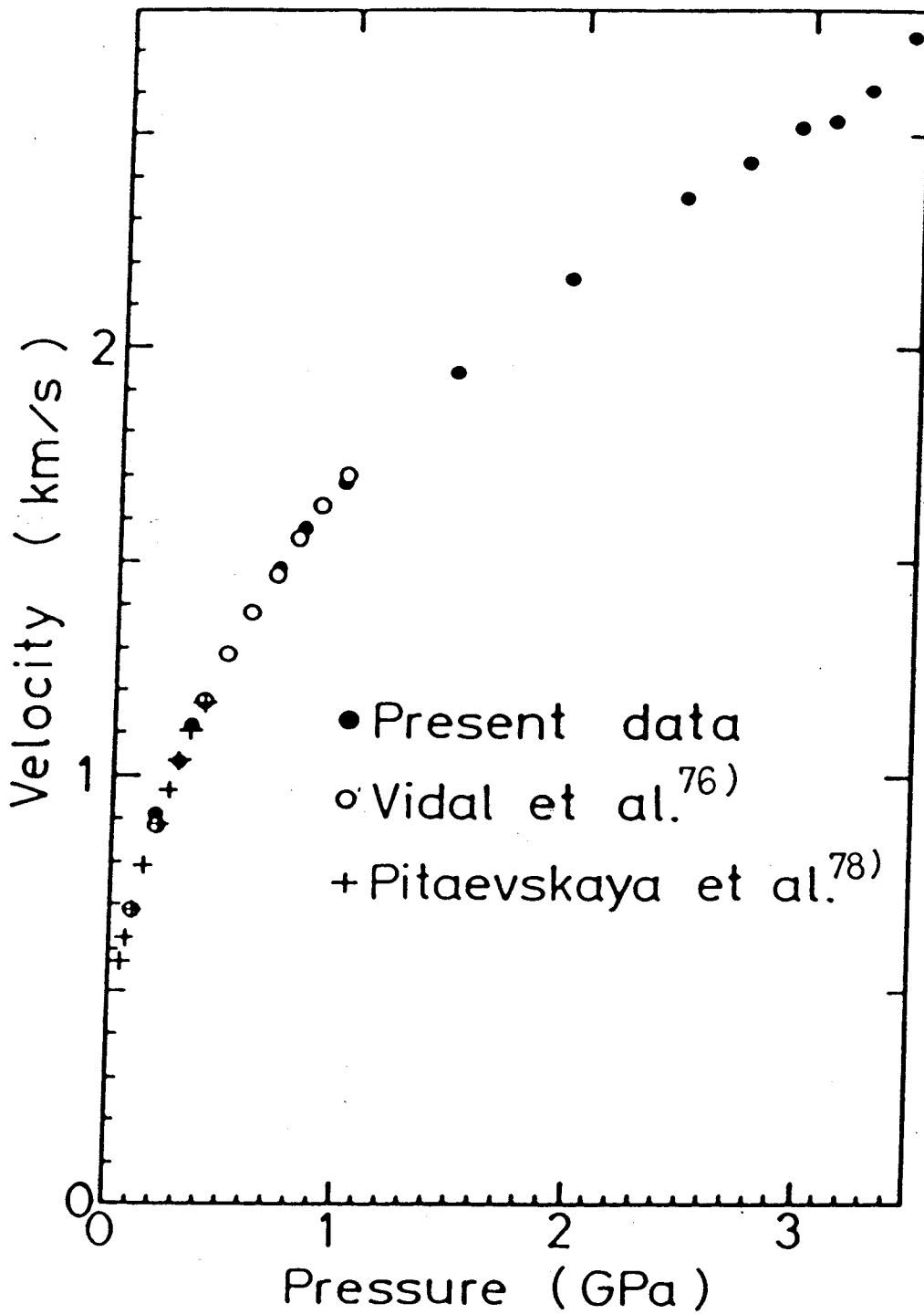


Fig. 21 Sound velocity versus pressure of neon at 22 °C.

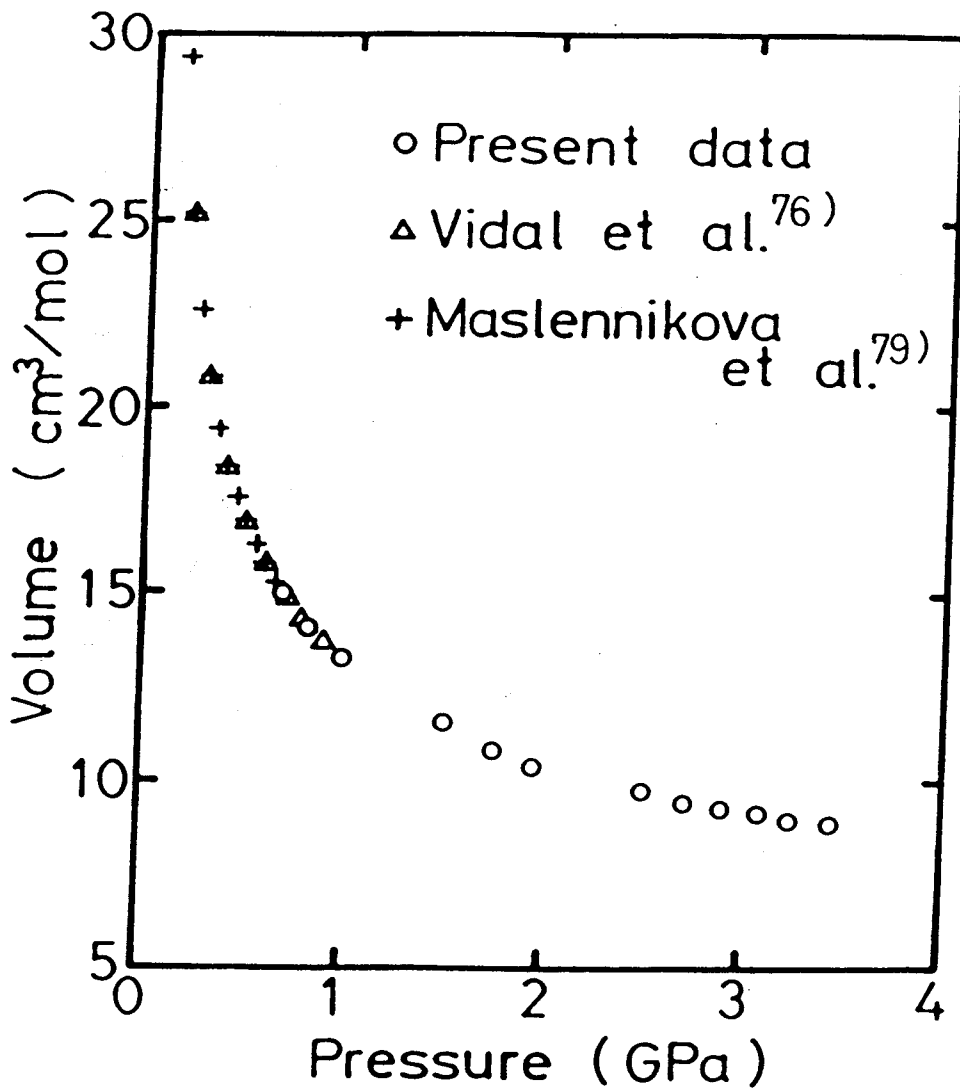


Fig. 22 Molar volume of neon gas as a function of pressure at 22 °C.

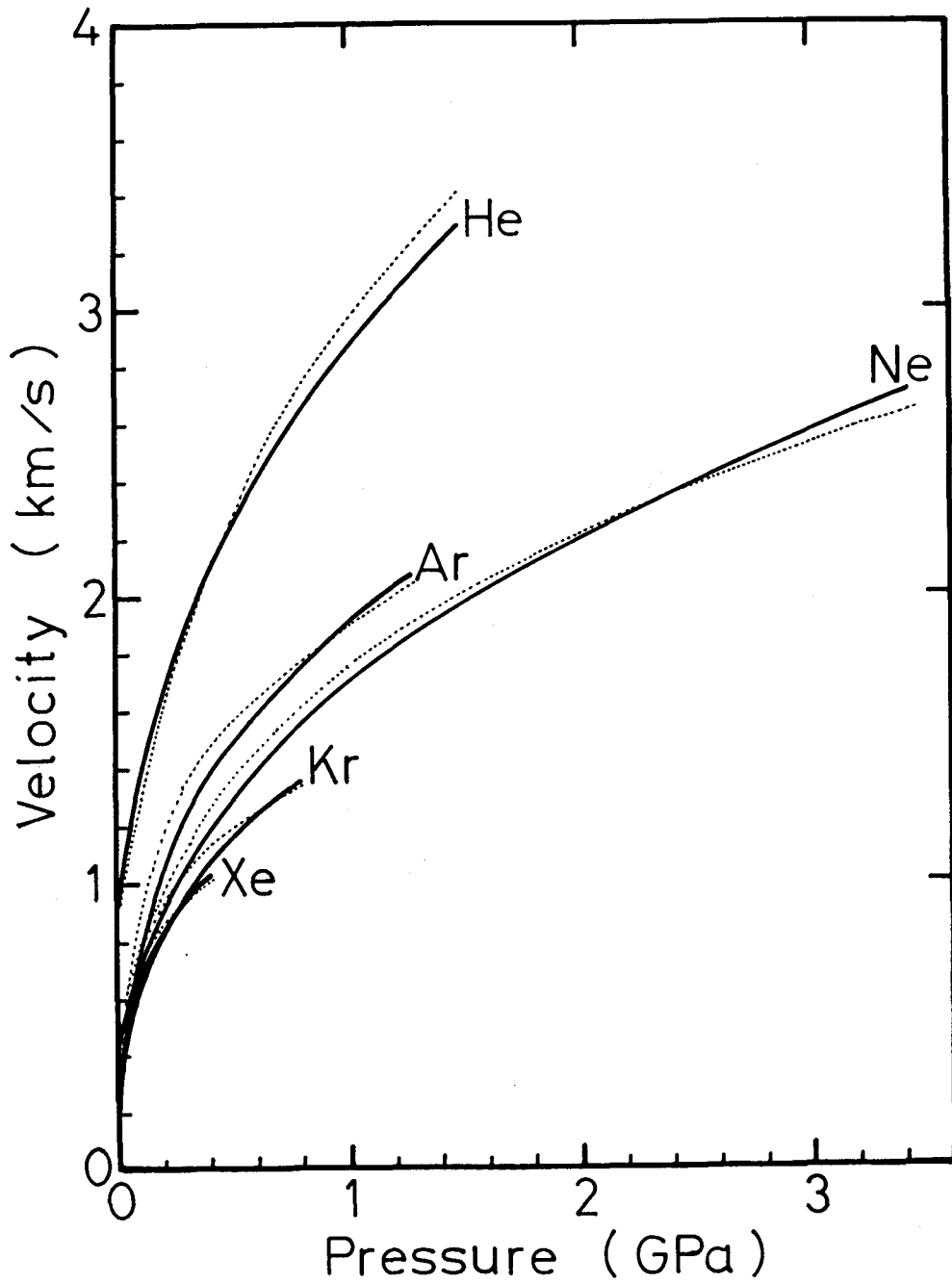


Fig. 23 Sound velocities of pure monoatomic gases at room temperature. Full lines are experimental data, and dotted lines are by the equation (8).

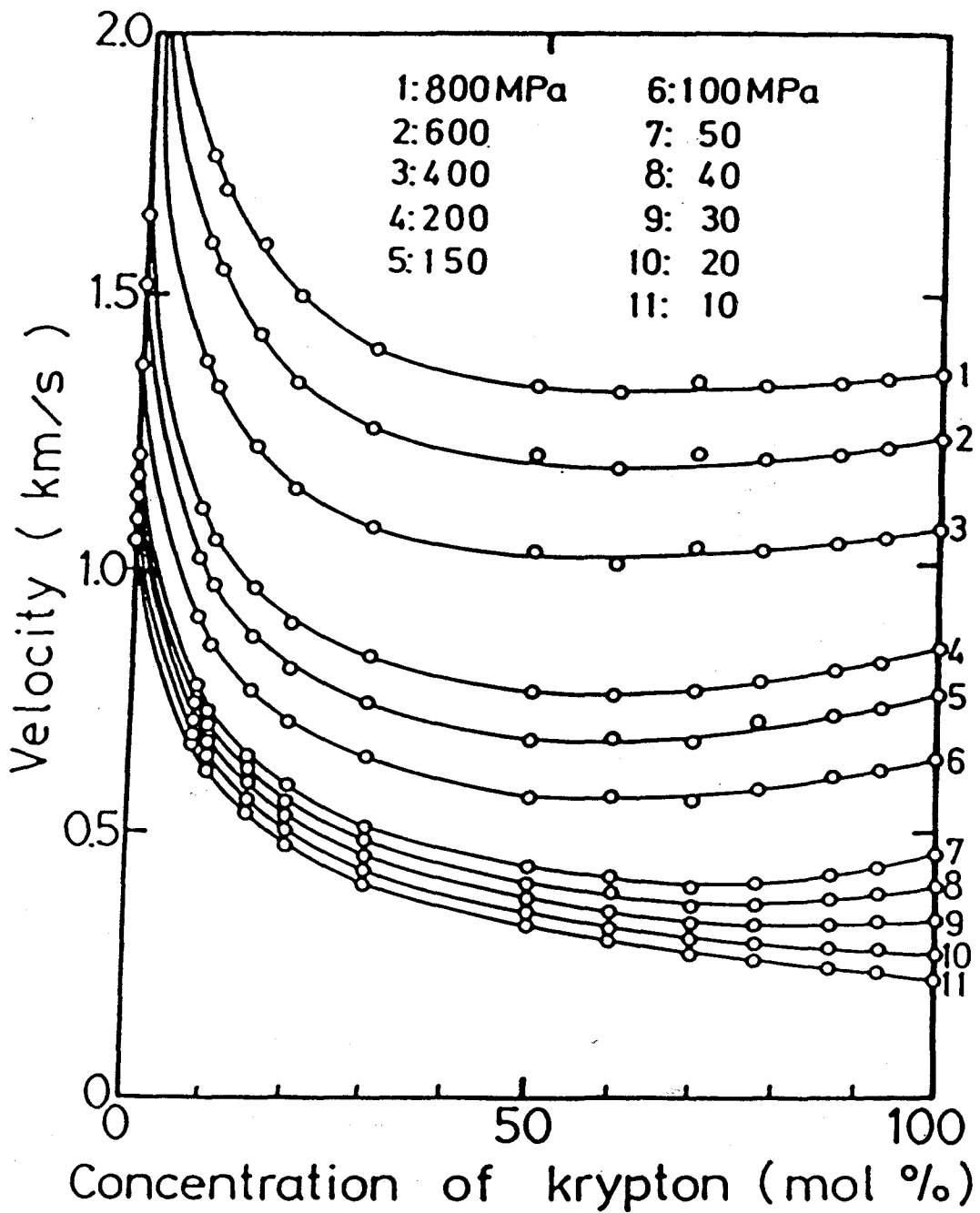


Fig. 24 Sound velocities in krypton-helium mixtures at various pressures as the functions of molar concentration of krypton at 20 °C.



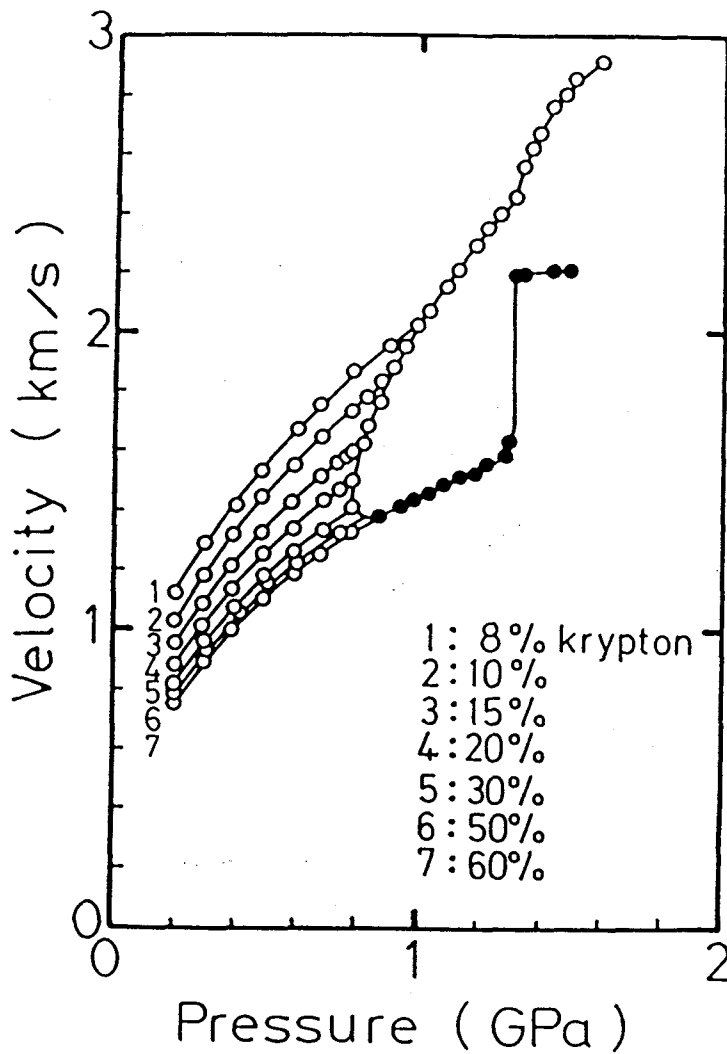


Fig. 25 Sound velocity changes in krypton-helium gas mixtures as the functions of pressure. Numbers from 1 to 7 correspond to 8, 10, 15, 20, 30, 50 and 60 percent krypton content.  $\circ$ : data from the upper chamber,  $\bullet$ : data from the lower chamber. An arrow shows the univariant three-phase separation point.

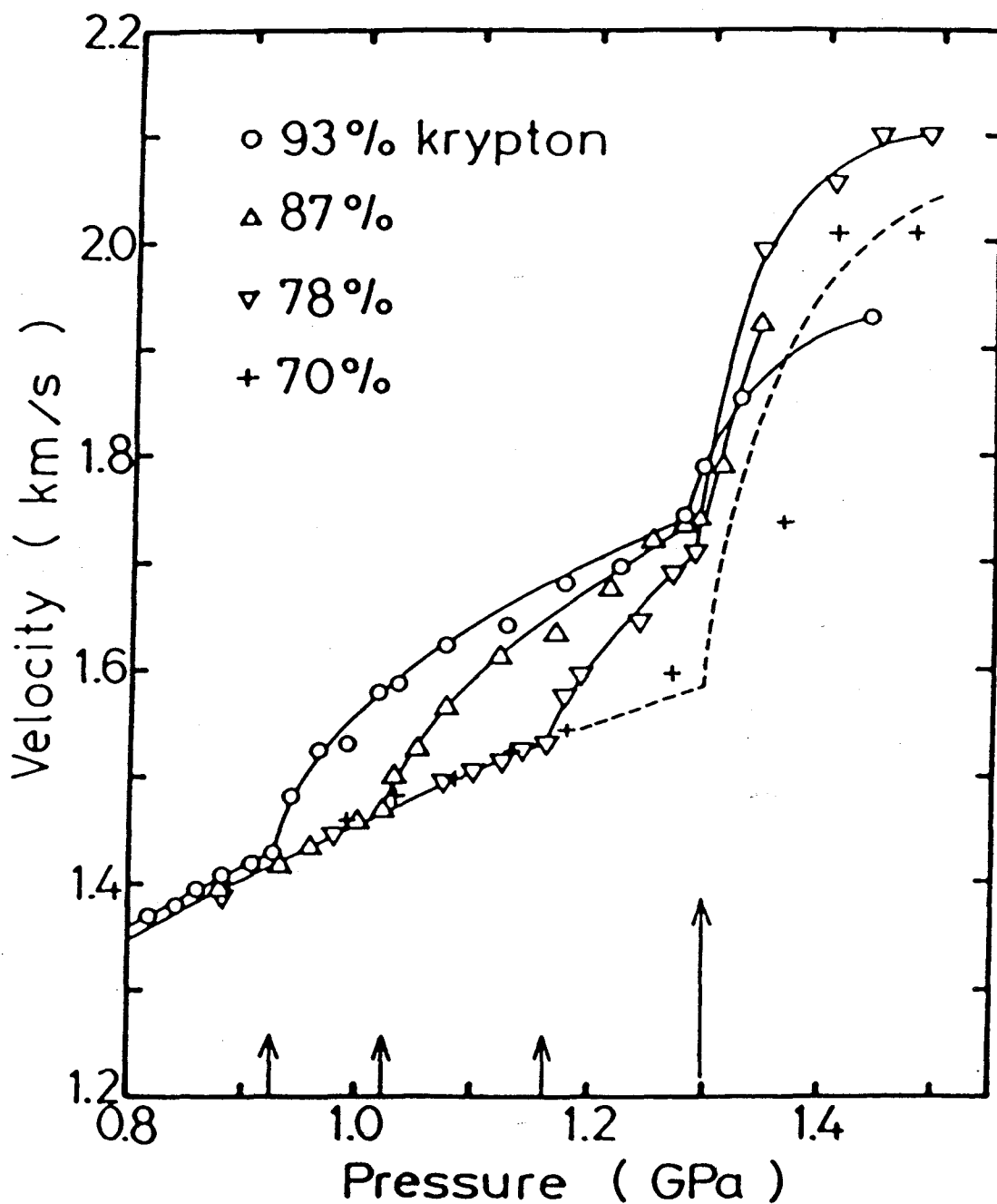


Fig. 26 Sound velocities in krypton-helium mixtures of 70, 78, 87 and 93 percent krypton, measured by the upper chamber at 20 °C. Short arrows show solidification points ( $G \rightarrow G+S$ ), and a long arrow shows the three-phase separation point ( $G+S \rightarrow G_1+G_2+S$ ).

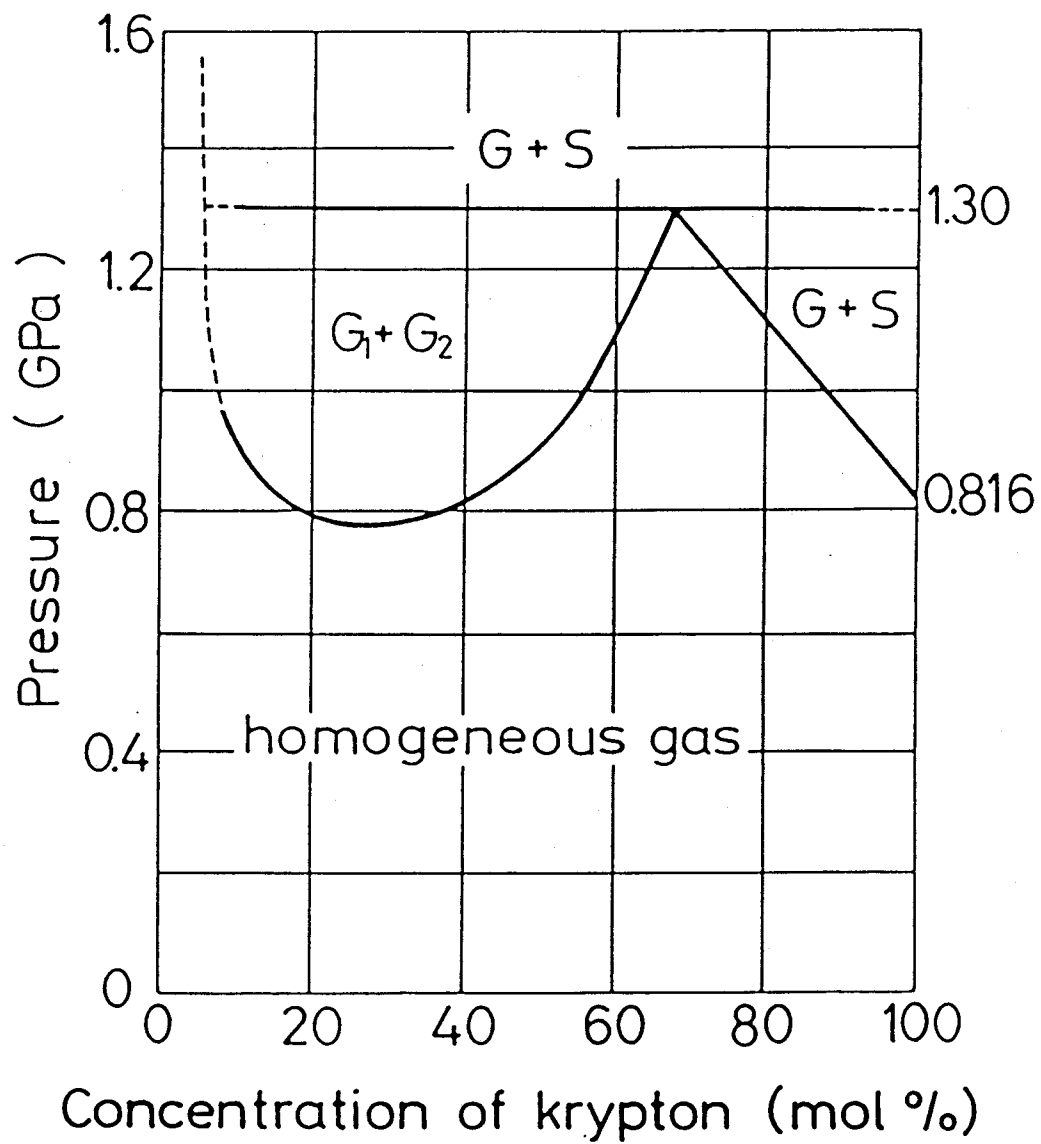


Fig. 27 Pressure-concentration phase diagram of krypton-helium at 20 °C. G and S mean the gas and solid phase, respectively.

## §6. Conclusion

Using the piston-cylinder high-pressure apparatus, neon gas was compressed up to 3.5 GPa without any trouble. It was also shown that the high-pressure vessel could be used repeatedly or almost indefinitely. Troublesome procedures such as re-honing the cylinder and revising the packings after each experiment were eliminated. There was no appreciable enlargement of the bore of the high pressure vessel up to 3.5 GPa. The new packing system solved the problem of leakage, but replacement of soft packings such as of Teflon, neoprene and bronze was still necessary after each experiment.

The velocities in nitrogen, krypton and neon gas were measured up to 2.6, 0.8 and 3.5 GPa at room temperature, respectively. The measurement offered precise and reproducible data, and the values obtained by other investigators were corrected. An empirical formula for the ultrasound velocities in rare gases,  $U = \sqrt{\gamma PV/M + (V_0/V)^2 b}$ , was proposed. The freezing points of nitrogen and krypton gas at room temperature were determined, as 2.329 GPa at 22 °C and 0.816 GPa at 20 °C, respectively, which were accurate enough to correct the scattered data published by other investigators. Using the two-chamber method, the transition pressures in the krypton-helium binary system could be determined without any ambiguity. The phase diagram of krypton-helium system at 20 °C was obtained by using the data of velocities of ultrasound waves in the range from 8 percent to 93 percent krypton content. The minimum pressure of the gas-gas phase separation was 0.78 GPa, at 27 percent krypton, and the univariant three-phase pressure was 1.30 GPa, where about

5 percent krypton gas phase, 68 percent krypton gas phase, and pure krypton solid phase were in equilibrium.

### Acknowledgements

The author would like to express his sincere thanks to Professor T. Nishitake for the promotion of this study and his continuous advice and encouragement. The author would like to express his cordial thanks to Professor F. E. Fujita of Osaka University for valuable discussions and reading the manuscript. He also thanks Dr. Y. Hanayama for many useful suggestions and helps throughout the experiments. He also thanks Professor S. Endo of Osaka University for his encouragement. He is also indebted to the members of the Professor Nishitake's Laboratory for their helps in the experiment, especially Mr. K. Oono. He also thanks Miss Y. Kataoka for her assistance through the present study.

This work was largely supported by a Grant-in-Aid for Special Equipment of Scientific Research from the Ministry of Education, Science and Culture.

## References

- 1) P. W. Bridgman: The Physics of High Pressure (Dover, New York, 1970): See also Collected Experimental Papers, 7 vols. (Harvard University Press, Cambridge, 1964).
- 2) W. R. D. Manning: Proc. 2nd Int. Conf. High Pressure Eng. Sussex, (1975), 101.
- 3) H. L. D. Pugh: The Mechanical Behaviour of Materials under Pressure (Elsevier Publishing, Amsterdam, 1970) p.391.
- 4) H. L. D. Pugh and C. J. H. Donaldson: High Pressure Technology, eds. I. L. Spain and J. Paauwe (Marcel Dekker, New York, 1977) vol. 2, p.423.
- 5) F. P. Bundy: Modern Very High Pressure Techniques, ed. R. H. Wentorf, (Butterworths, London, 1962) Chap. 1, p.1.
- 6) P. W. Bridgman: Proc. Amer. Acad. Arts and Sci. 74 (1940) 1.
- 7) F. R. Boyd and J. L. Engrand: J. Geophys. Res., 65 (1960) 741.
- 8) F. R. Boyd: Modern Very High Pressure Techniques, ed. R. H. Wentorf, (Butterworths, London, 1962) Chap. 8, p.151.
- 9) N. Keeler: High Pressure in Reserch and Industry, eds. C. M. Backman, T. Johannisson and L. Tegner, (Arkitektkopa, Uppsala, Sweden, 1982)
- 10) J. C. Haygarth, I.C. Getting and G. C. Kennedy: J. Appl. Phys., 38 (1967) 4557.
- 11) J. C. Haygarth and G. C. Kennedy: Rev. Sci. Instr. 38 (1967) 1590.
- 12) P. W. Bridgman: Proc. Amer. Acad. Arts and Sci. 81 (1952) 165.
- 13) A. S. Balchan and H. G. Drickamer: Rev. Sci. Inst., 32 (1961)

308.

- 14) F. P. Bundy: *Rev. Sci. Inst.*, **46** (1975) 131.
- 15) F. P. Bundy: *Rev. Sci. Inst.*, **51** (1980) 753.
- 16) J. C. Jamieson and A. W. Lawson: *Rev. Sci. Inst.*, **30** (1959) 1016.
- 17) J. C. Jamieson and A. W. Lawson: *Modern Very High Pressure Techniques*, ed. R. H. Wentorf, (Butterworths, London, 1962) Chap. 4, p.70.
- 18) C. E. Weir, E. R. Lippincott, A. Van Valkenburg and E. N. Bunting: *J. Res. Natn. Bur. Stand.* **A63** (1959) 55.
- 19) C. E. Weir, A. van Valkenburg and E. R. Lippincott: *Modern Very High Pressure Techniques*, ed. R. H. Wentorf, (Butterworths, London, 1962) Chap. 3, p.51.
- 20) J. A. Schouten, L. C. Van Den Bergh and N. J. Trappeniers: *High Pressure in Science and Technology*, eds. C. Homan, R. K. MacCrone and E. Whalley (North-Holland, New York, 1984) part II, p. 73.
- 21) H. K. Mao, P. M. Bell, K. J. Dunn, R. M. Chrenko and R. C. de Vries: *Rev. Sci. Inst.*, **50** (1979) 1002.
- 22) H. T. Hall: *Rev. Sci. Instr.*, **31** (1960) 125.
- 23) H. T. Hall: *Rev. Sci. Instr.*, **29** (1958) 267.
- 24) L. F. Vereshchagin: *Progress in Very High Pressure Reserch*, eds. F. P. Bundy, W. R. Hibbard and H. M. Strong (John Wiley and Sons, New York, 1961) p 290.
- 25) J. C. Houck and U. O. Hutton: *High Pressure Measurements*, eds. A. A. Giardini and E. C. Lloyd (Butterworths, Washington, 1963) p. 221.
- 26) E. C. Lloyd, U. O. Hutton and D. P. Johnson: *J. Res. Natn.*



- Bur. Stand., C63 (1959) 59.
- 27) B. Van Platen: Modern Very High Pressure Techniques, ed. R. H. Wentorf, (Butterworths, London, 1962) Chap. 6, p.118.
- 28) N. Kawai: Accurate Characterization of the High Pressure Environment, ed. E. C. Lloyd, (National Bureau of Standard, Washington, DC, NBS Special Publication 326, 1971) p.45.
- 29) N. Kawai and S. Endo: Rev. Sci.Instr., 41 (1970) 1178.
- 30) N. Kawai and S. Mochizuki: Sol. State Commun., 9 (1971) 1393.
- 31) R. Epain, C. Susse and B. Voder: C.r. hebd. Seanc. Acad. Sci., Paris, 265 (1967) 323.
- 32) R. Epain, G. Bocquillon, C. Loriers-Susse and J. Loriers: Rev. Sci.Instr., 51 (1980) 983.
- 33) M. Kumazawa: High Temp.-High Press., 3 (1971) 243.
- 34) M. Kumazawa, K. Masaki, H. Sawamoto and M. Kato: High Temp.-High Press., 4 (1972) 293.
- 35) M. Kumazawa and N. Nakahama: Rev. Sci.Instr., 46 (1975) 84.
- 36) F. Birch and E. C. Robertson: Office of Naval Research Final Report N5 ori-07644 (1957).
- 37) D. S. Hughes and T. Nishitake: Geophysical Papers Dedicated to Prof. K. Sassa (Geophysical Institute, Kyoto Univ., Kyoto, 1963) p. 379.
- 38) T. Nishitake and Y. Hanayama: Proc. 4th Int. Conf. High Pressure, Kyoto, 1974 (Physico-chemical Society of Japan, Kyoto, 1974) p. 534.
- 39) D. H. Newhall: Ind. Eng. Chem., 49 (1957) 1993.
- 40) D. H. Liebenberg, R. L. Mills and J. C. Bronson: J. Appl. Phys. 45 (1974) 741.
- 41) A. Lavergne and E. Whalley: Rev. Sci. Instrum. 49 (1978) 923.

- 42) M. Kimura, Y. Hanayama and T. Nishitake: Jpn. J. Appl. Phys. 38 (1987) 1361.
- 43) R. L. Mills, D. H. Liebenberg and J. C. Bronson: J. Chem. Phys. 63 (1975) 1198.
- 44) R. L. Mills, D. H. Liebenberg and J. C. Bronson: J. Chem. Phys. 63 (1975) 4026.
- 45) R. L. Mills, D. H. Liebenberg, J. C. Bronson and L. C. Schmidt: J. Chem. Phys. 55 (1977) 3076.
- 46) D. H. Liebenberg, R. L. Mills and J. C. Bronson: Phys. Rev. B 18 (1978) 4526.
- 47) R. L. Mills, D. H. Liebenberg and J. C. Bronson: J. Appl. Phys. 49 (1978) 5502.
- 48) R. L. Mills, D. H. Liebenberg and J. C. Bronson: J. Chem. Phys. 68 (1978) 2663.
- 49) R. L. Mills, D. H. Liebenberg and J. C. Bronson: Phys. Rev. B 21 (1980) 5137.
- 50) R. L. Mills, D. H. Liebenberg and Ph. Pruzan: J. Phys. Chem. 86 (1982) 5219.
- 51) Ph. Pruzan, D. H. Liebenberg and R. L. Mills: Phys. Rev. Lett. 48 (1982) 1200.
- 52) J. D. van der Waals: Zittinsversl. Kon. Akad. Wetensch. Amsterdam., (1894) 133.
- 53) H. Kamerlingh Onnes and W. H. Keesom: Commun. Phys. Lab. Univ. Leiden, Suppl. No. 15 (1907); Proc. Roy. Acad. Sci. Amst. 9, (1907) 786; 10 (1907) 231.
- 54) I. R. Krichevskii: Acta Phys. Chim. URSS, 12 (1940) 480.
- 55) I. R. Krichevskii: Intern. Cong. Pure Appl. Chem. 17th, Munchen 1959, Vol. 2 (1960)

- 56) J. De Swaan Arons: Thesis. Delft, 1963.
- 57) J. De Swaan Arons and G. A. M. Diepen: J. Chem. Phys. 44  
(1966) 2322.
- 58) G. M. Schneider: Adv. Chem. Phys. 17 (1970) 1.
- 59) W. B. Streett: Can. J. Chem. Eng. 52 (1974) 92.
- 60) D. S. Tsiklis: Russ. J. Phys. Chem. 50 (1976) 825.  
translation: Zh. Fiz. Khim. 50 (1976) 1361.
- 61) G. F. Molinar, V. Bean, J. Houck and B. Welch: Metrologia  
16 (1980) 21.
- 62) G. N. Peggs and R. Wisniewski: High Pressure Measurement  
Techniques, ed. G. N. Peggs (Applied Science Publishers, New  
York, 1983) Chap. 6, p. 223.
- 63) A. L. Ruoff, R. C. Lincoln and Y. C. Chen: J. Phys. D, 6  
(1973) 1295.
- 64) H. J. McSkimin: J. Acoust. Soc. Am. 33 (1961) 12.
- 65) M. Kimura, Y. Hanayama and T. Nishitake: Jpn. J. Appl. Phys.  
38 (1987) 1366.
- 66) D. S. Hughes, T. Nishitake and J. P. Doty: Appl. Phys. Lett.  
3 (1963) 119.
- 67) V. M. Cheng, W. B. Daniels and R. K. Crawford: Phys. Rev.  
B 11 (1975) 3972.
- 68) P. H. Lahr and W. G. Eversole: J. Chem. Eng. Data 7 (1962)  
42.
- 69) R. K. Crawford and W. B. Daniels: J. Chem. Phys. 55 (1971)  
5651.
- 70) Y. Hanayama: J. Phys. Soc. Japan 46 (1979) 328.
- 71) A. E. H. Love: A Treatise on the Mathematical Theory of  
Elasticity, (Cambridge Univ. Press, London, 1927) Chap. 5,

p. 144.

- 72) R. Hill: The Mathematical Theory of Plasticity, (Clarendon Press, Oxford, 1950) Chap. 5, p. 97.
- 73) E. C. Morris and R. G. Wylie: J. Chem. Phys. 79 (1983) 2982.
- 74) N. J. Trappeniers, T. Wassenaar and G. J. Wolkers: Physica 32 (1966) 1503.
- 75) F. F. Voronov, L. L. Pitaevskaya and A. V. Bilevich: Russ. J. Phys. Chem. 43 (1969) 321.
- 76) D. Vidal, R. Tufeu, Y. Garrabos and B. Le Neindre: High Pressure Science and Technology, eds. B. Vodar and Ph. Marteau (Pergamon, Paris, 1980) Vol. 2, p. 692.
- 77) G. Zou, H. K. Mao, L. W. Finger, P. M. Bell and R. M. Hazen: Physics of Solids under High Pressure, eds. J. S. Schilling and R. N. Shelton (North-Holland, New York, 1981) p.137
- 78) L. L. Pitaevskaya and A. V. Bilevich: High Temp.-High Pressure 5 (1973) 459.
- 79) V. Y. Maslennikova, A. N. Egorov and D. S. Tsiklis: Dokl. Akad. Nauk SSSR 229 (1976) 827 [in Russian.]
- 80) W. Van Dael and A. Van Itterbeek: Physics of High Pressures and the Condensed Phase, ed. A. Van Itterbeek (North-Holland, Amsterdam, 1965) Chap. 7, p. 338.
- 81) D. H. Liebenberg, R. L. Mills and J. C. Bronson: Los Alamos Scientific Laboratory report LA-6645-MS (1977).
- 82) T. Takagi: J. Chem. Thermodynamics. 12 (1980) 277.
- 83) T. Nishitake and Y. Hanayama: J. Phys. Soc. Japan 39 (1975) 1065.
- 84) A. J. Kidnay, R. C. Miller and M. J. Hiza: Ind. Eng. Chem. Fundam, 10 (1971) 459.

85) D. D. Dillard, M. Waxman and R. L. Robinson: J. Chem. Eng.  
Data 23 (1978) 269.